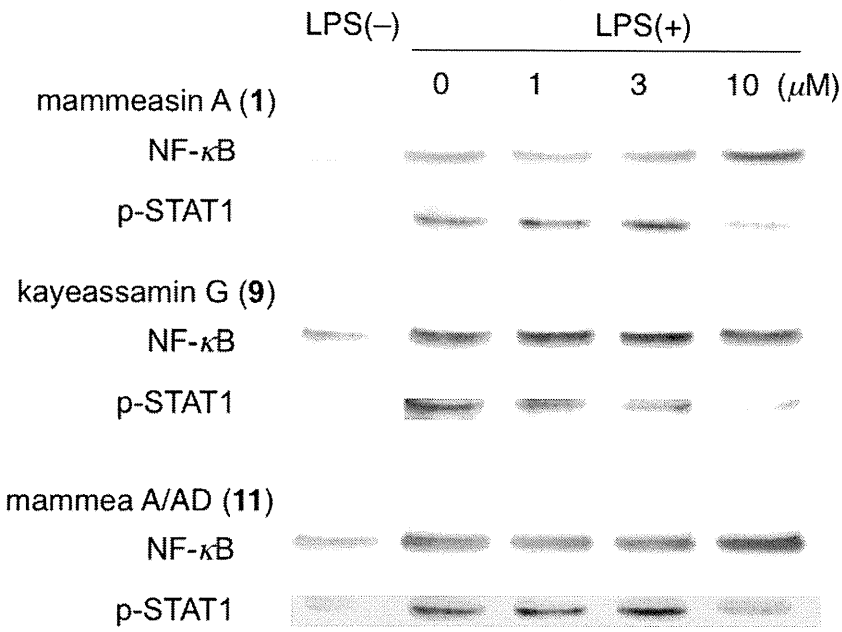

Figure 5. Effects of **1**, **9**, and **11** on nuclear protein levels of NF-κB and p-STAT1.

−2.4 ± 1.1% inhibition at 100 μM and 7.2 ± 2.2% inhibition at 10 μM, respectively. While a JNK inhibitor (SP600125) significantly inhibited the production of NO (74.6 ± 0.6% inhibition at 30 μM, IC_{50} = 17 μM) consistent with the previous report by Lin et al.[65] Furthermore, an inhibitor of phosphorylation of p38, SB202190, showed significant inhibition (IC_{50} = ca. 16 μM) (Table 4). These findings suggested that phosphorylations of JNK and p38 are important steps for expression of iNOS under our experimental conditions. However, in the present study, the active coumarins (**1**, **9**, and **11**) did not inhibit the phosphorylations of these MAP kinases (Fig. 6).

Signal transducer and activator of transcription-1 (STAT1) as well as NF-κB are also important nuclear factor for iNOS expression, and STAT1 is known to activate by IFNβ or IFNγ. Transcription of IFNβ by LPS via Toll-like receptor-4 (TLR4) is reported to be independent of activation of NF-κB, but LPS induce the IFNβ via activation of IFN-regulatory factor-3 (IRF3) in macrophages. The STAT1 is phosphorylated and translocated into the nucleus to activate transcription of its target genes including iNOS.[67–69] Therefore, in the present study, effects of **1**, **9**, and **11**, on phosphorylated STAT1 (p-STAT1) in the nuclear protein fraction were examined. As a result, the protein levels of p-STAT1 in nuclear protein fraction were reduced by **1**, **9**, and **11** in a concentration-dependent manner (Fig. 5). These findings suggest that inhibition of STAT1 activation is mainly involved in the inhibitory effects on iNOS expression by **1**, **9**, and **11**. The detailed mechanism of action including the difference in cytotoxic effects should be studied further.

3. Experimental

3.1. General

The following instruments were used to obtain spectral and physical data: specific rotations, Horiba SEPA-300 digital polarimeter (l = 5 cm); UV spectra, Shimadzu UV-1600 spectrometer; IR spectra, Shimadzu FTIR-8100 spectrometer; ^{1}H NMR spectra, JEOL JNM-ECA700 (700 MHz), JNM-ECA600 (600 MHz), and JNM-ECS400 (400 MHz) spectrometers; ^{13}C NMR spectra, JEOL JNM-ECA700 (175 MHz), JNM-ECA600 (150 MHz), and JNM-ECS400 (100 MHz) spectrometers with tetramethylsilane as an internal standard; EIMS and HREIMS, JEOL JMS-GCMATE mass spectrometer; FABMS and HRFABMS, JEOL JMS-SX 102A mass spectrometer; HPLC detector, Shimadzu SPD-10A UV–VIS detector (230 nm); HPLC column, Cosmosil 5C_{18}-MS-II and πNAP (250 × 4.6 mm i.d. and 250 × 20 mm i.d. for analytical and preparative purposes, respectively).

The following experimental conditions were used for chromatography (CC): highly porous synthetic resin, Diaion HP-20 (Mitsubishi Chemical, Tokyo, Japan); normal-phase silica gel CC, silica gel 60N (Kanto Chemical Co., Ltd., Tokyo, Japan; 63–210 mesh, spherical, neutral); reversed-phase ODS CC, Chromatorex ODS DM1020T (Fuji Silysia Chemical, Ltd., Aichi, Japan; 100–200 mesh); TLC, pre-coated TLC plates with silica gel 60F_{254} (Merck, 0.25 mm) (normal-phase) and silica gel RP-18 F_{254S} (Merck, 0.25 mm) (reversed-phase); reversed-phase HPTLC, pre-coated TLC plates with silica gel RP-18 WF_{254S} (Merck, 0.25 mm), detection was achieved by spraying with 1% $Ce(SO_4)_2$–10% aqueous H_2SO_4, followed by heating.

3.2. Plant material

The flower of *M. siamensis* was collected in Nakhonsithammarat Province, Thailand on September 2006. The plant material was identified by one of the authors (Y.P.). A voucher specimen (2006.09. Raj-04) of this plant is on file in our laboratory.

3.3. Extraction and isolation

Dried flowers of *M. siamensis* (1.8 kg) were extracted three times with MeOH under reflux for 3 h. Evaporation of the combined extracts under reduced pressure provided a MeOH extract (463.7 g, 25.66%). An aliquot (413.7 g) was partitioned into an EtOAc–H_2O (1:1, v/v) mixture to furnish an EtOAc-soluble fraction (110.34 g, 6.84%) and an aqueous phase. The aqueous phase was subjected to Diaion HP-20 CC (2.4 kg, H_2O → MeOH, twice) to give H_2O-eluted (217.70 g, 13.50%) and MeOH-eluted (68.10 g, 4.22%) fractions, respectively. An aliquot (89.45 g) of the EtOAc-soluble fraction was subjected to normal-phase silica gel CC [3.0 kg, *n*-hexane–EtOAc (10:1 → 7:1 → 5:1, v/v) → EtOAc → MeOH] to give 11 fractions [Fr. 1 (3.05 g), Fr. 2 (2.86 g), Fr. 3 (11.71 g), Fr. 4 (1.62 g), Fr. 5 (4.15 g), Fr. 6 (6.29 g), Fr. 7 (2.21 g), Fr. 8 (2.94 g), Fr. 9 (10.23 g), Fr. 10 (11.17 g), and Fr. 11 (21.35 g)]. The fraction

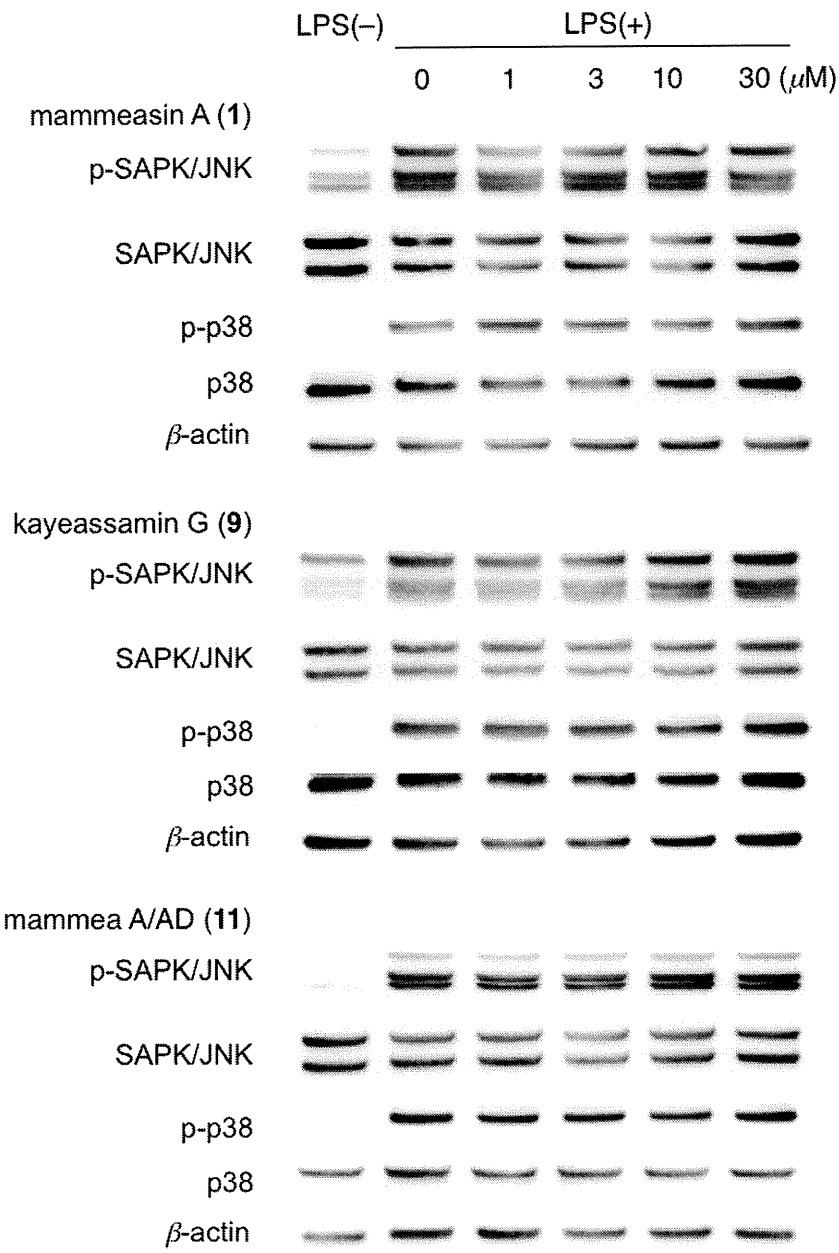

Figure 6. Effects of **1**, **9**, and **11** on SAPK/JNK, p-SPK/JNK, p-p38, and p38 protein levels.

3 (11.71 g) was subjected to reversed-phase ODS CC [340 g, MeOH–H_2O (90:10 → 95:5, v/v) → MeOH → acetone] to afford seven fractions [Fr. 3–1 (49.3 mg), Fr. 3–2 (3109.8 mg), Fr. 3–3 (4679.3 mg), Fr. 3–4 (1089.1 mg), Fr. 3–5 (1034.0 mg), Fr. 3–6 (280.8 mg), and Fr. 3–7 (85.6 mg)]. The fraction 3–4 (497.9 mg) was purified by HPLC [Cosmosil $5C_{18}$-MS-II, MeOH–1% aqueous AcOH (90:10, v/v)] to give mammea A/AB cyclo D (**12**, 27.8 mg, 0.0047%), mammea A/AC cyclo D (**13**, 46.0 mg, 0.0077%), mammea B/AB cyclo D (**14**, 9.8 mg, 0.0016%), and mammea B/AC cyclo D (**15**, 32.9 mg, 0.0055%). The fraction 3–5 (502.8 mg) was purified by HPLC [Cosmosil $5C_{18}$-MS-II, MeOH–1% aqueous AcOH (95:5, v/v)] to give surangins C (**4**, 8.2 mg, 0.0013%) and D (**5**, 24.9 mg, 0.0039%), and β-amyrin (46.0 mg, 0.0072%). The fraction 6 (6.29 g) was subjected to reversed-phase ODS CC [200 g, MeOH–H_2O (80:20 → 90:10 → 95:5, v/v) → MeOH → acetone] to afford 10 fractions [Fr. 6–1 (44.7 mg), Fr. 6–2 (157.2 mg), Fr. 6–3 (928.8 mg), Fr. 6–4 (3117.0 mg), Fr. 6–5 (128.8 mg), Fr. 6–6 (487.1 mg), Fr. 6–7 (230.8 mg), Fr. 6–8 (280.5 mg), Fr. 6–9 (102.9 mg), and Fr. 6–10 (96.5 mg)]. The fraction 6–3 (514.6 mg) was purified by HPLC [Cosmosil $5C_{18}$-MS-II, MeOH–1% aqueous AcOH (80:20, v/v)] to give mammea A/AC (**10**, 35.6 mg, 0.0049%), mammea A/AD (**11**, 15.8 mg, 0.0022%), and mammea E/BB (**16**, 140.1 mg, 0.0194%). The fraction 6–4 (536.2 mg) was purified by HPLC [Cosmosil $5C_{18}$-MS-II, MeOH–1% aqueous AcOH (90:10, v/v)] to give mammeasins A (**1**, 65.8 mg, 0.0293%) and B (**2**, 21.6 mg, 0.0096%), surangin B (**3**, 58.2 mg, 0.0259%), and **10** (112.6 mg, 0.0501%). The fraction 6–5 (128.8 mg) was purified by HPLC [Cosmosil $5C_{18}$-MS-II, MeOH–1% aqueous AcOH (90:10, v/v)] to give **2** (24.1 mg, 0.0019%) and **3** (15.1 mg, 0.0012%). The fraction 6–6 (487.1 mg) was purified by HPLC [Cosmosil $5C_{18}$-MS-II, MeOH–1% aqueous AcOH (90:10, v/v)] to give **10** (6.0 mg, 0.00050%). The fraction 9 (10.23 g) was subjected to reversed-phase ODS CC [300 g, MeOH–H_2O (80:20 → 90:10, v/v) → MeOH → acetone] to afford five fractions [Fr. 9–1 (2809.0 mg), Fr. 9–2 (5678.0 mg), Fr. 9–3 (385.9 mg), Fr. 9–4 (422.0 mg), and Fr. 9–5 (51.9 mg)]. The fraction 9–1 (544.5 mg) was purified by HPLC [Cosmosil $5C_{18}$-MS-II, MeOH–1% aqueous AcOH (85:15, v/v)] to give kayeassamins E (**7**, 28.6 mg, 0.0113%),

F (**8**, 98.7 mg, 0.0390%), and G (**9**, 43.4 mg, 0.0171%), deacetylmammea E/BC cyclo D (**17**, 18.6 mg, 0.0073%), and benzoic acid (10.9 mg, 0.0043%). The fraction 9–2 (526.2 mg) was purified by HPLC [Cosmosil $5C_{18}$-MS-II, MeOH–1% aqueous AcOH (90:10, v/v)] to give **4** (63.6 mg, 0.0525%), **5** (66.7 mg, 0.0551%), and kayeassamin A (**6**, 68.1 mg, 0.0562%). The fraction 9–3 (385.9 mg) was purified by HPLC [Cosmosil $5C_{18}$-MS-II, MeOH–1% aqueous AcOH (90:10, v/v)] to give **4** (43.1 mg, 0.0033%), **5** (54.3 mg, 0.0042%), and **6** (20.5 mg, 0.0016%).

3.3.1. Mammeasin A (1)

Pale yellow oil, $[\alpha]_D^{27}$ −29.7 (*c* 1.08, MeOH), $[\alpha]_D^{27}$ −25.4 (*c* 1.08, $CHCl_3$). EIMS (*m/z*, %): 484 (M^+, 7), 301 (100). High-resolution EIMS: Anal. Calcd for $C_{28}H_{36}O_7$ (M^+): 484.2461. Found: 484.2466. UV [MeOH, nm (log ε)]: 223 (4.62), 330 (4.65). IR (film): 3503, 1748, 1717, 1609, 1458, 1399, 1233, 1194, 1136 cm^{-1}. ^1H NMR (700 MHz, $CDCl_3$) δ: given in Table 2. ^{13}C NMR (175 MHz, $CDCl_3$) δ_C: given in Table 3.

3.3.2. Mammeasin B (2)

Pale yellow oil, $[\alpha]_D^{27}$ −19.2 (*c* 0.30, MeOH), $[\alpha]_D^{26}$ −18.4 (*c* 0.30, $CHCl_3$). EIMS (*m/z*, %): 498 (M^+, 8), 315 (100). High-resolution EIMS: Anal. Calcd for $C_{29}H_{38}O_7$ (M^+): 498.2618. Found: 498.2622. UV [MeOH, nm (log ε)]: 223 (4.48), 331 (4.58). IR (film): 3500, 1744, 1719, 1607, 1458, 1404, 1233, 1196, 1132 cm^{-1}. ^1H NMR (700 MHz, $CDCl_3$) δ: given in Table 2. ^{13}C NMR (175 MHz, $CDCl_3$) δ_C: given in Table 3.

3.4. Acetylation of surangin D (5) and kayeassamin A (6)

To a solution of **5** (4.5 mg) in pyridine (1.0 mL) was added Ac_2O (0.8 mL), and the mixture was stirred at room temperature for 24 h. The reaction mixture was poured into water and the resulting mixture was extracted with EtOAc. The extract was washed with 5% aqueous HCl, saturated aqueous $NaHCO_3$, and brine, then dried over anhydrous $MgSO_4$ and filtered. Removal of the solvent under reduced pressure gave a pale yellow oil, which was purified by HPLC [Cosmosil $5C_{18}$-MS-II, MeOH–1% aqueous AcOH (90:10, v/v)] to furnish **1** (4.3 mg, 88%). According to the similar procedure, **2** (4.2 mg, quant.) was obtained from **6** (3.6 mg).

3.5. Preparation of (*R*)-MTPA ester (5a) and (*S*)-MTPA ester (5b) from surangin D (5)

A solution of **5** (2.3 mg) in pyridine (1.0 mL) was treated with (*S*)-(+)-α-methoxy-α-(trifluoromethyl)phenylacetic chloride [(*S*)-(+)-MTPA-Cl, 7.5 μL] and the mixture was stirred at room temperature for 24 h. The reaction mixture was poured into ice-water and extracted with EtOAc. The extract was successively washed with 5% aqueous HCl, saturated aqueous $NaHCO_3$, and brine, then dried over anhydrous $MgSO_4$ and filtered. Removal of the solvent from the filtrate under reduced pressure furnished a pale yellow oil, which was purified by HPLC [Cosmosil $5C_{18}$-MS-II, MeOH–1% aqueous AcOH (90:10, v/v)] to give the (*R*)-MTPA ester derivative (**5a**, 0.9 mg, 26%). According to the similar procedure, **5b** (0.5 mg, 14%) was obtained from **5** (2.5 mg) by using (*R*)-(−)-MTPA-Cl (7.5 μL).

3.5.1. Compound 5a

^1H NMR (400 MHz, $CDCl_3$) δ: 1.03 (6H, d, *J* = 6.8 Hz, H_3-4‴, 5‴), 1.05 (3H, t, *J* = 6.8 Hz, H_3-1″), 1.61 (3H, br s, H_3-10″), 1.68 (3H, br s, H_3-9″), 1.77, 2.01 (1H each, both m, H_2-2′), 1.88 (3H, br s, H_3-5″), 3.49 (3H, s, $-OCH_3$), 5.07 (1H, br t-like, H-7″), 5.27 (1H, br dd-like, H-2″), 5.63 (1H, dd-like, H-1′), 5.83 (1H, br s, H-3) [7.45 (3H, m), 7.52 (2H, m), Ph-H].

3.5.2. Compound 5b

^1H NMR (400 MHz, $CDCl_3$) δ: 1.04 (3H, t, *J* = 6.6 Hz, H_3-1″), 1.06 (6H, d, *J* = 6.6 Hz, H_3-4‴, 5‴), 1.60 (3H, br s, H_3-10″), 1.64 (3H, br s, H_3-9″), 1.76 (3H, br s, H_3-5″), 1.76, 2.00 (1H each, both m, H_2-2′), 3.49 (3H, s, $-OCH_3$), 5.06 (1H, br t-like, H-7″), 5.27 (1H, br dd-like, H-2″), 5.64 (1H, dd-like, H-1′), 5.88 (1H, br s, H-3) [7.46 (3H, m), 7.54 (2H, m), Ph-H].

3.6. Bioassay

3.6.1. Cell culture

The murine macrophage cells (RAW264.7, ATCC No. TIB-71) were obtained from Dainippon Pharmaceutical, Osaka, Japan and cultured in Dulbecco's modified Eagle's medium (DMEM, containing 4500 mg/L glucose) supplemented with 10% fetal bovine serum (FBS), penicillin (100 U/mL), and streptomycin (100 μg/mL) (Sigma Chemical Co., St. Louis, MO, USA). The cells were incubated at 37 °C in 5% CO_2/air.

3.6.2. Effects on production of NO in LPS-stimulated macrophage RAW264.7 cells

The total amount of nitrite in a medium is used as an indicator of NO synthesis.[59] The screening test for NO production using RAW264.7 cells was described previously.[58,59] Briefly, RAW264.7 cells were cultured in DMEM, and the suspension of the cells were seeded into a 96-well microplate at 2.5×10^5 cells/100 μL/well. After 6 h, nonadherent cells were removed by washing with PBS, and the adherent cells were cultured in 100 μL of fresh medium containing the test compounds for 10 min, and then 100 μL of the medium containing LPS (from *Escherichia coli*, 055: B5, Sigma) was added to stimulate the cells for 18 h (final concentration of LPS was 10 μg/mL). The nitrite concentration was measured from the supernatant by Griess reaction. Inhibition (%) was calculated using the following formula and the IC_{50} was determined graphically ($N = 4$). Caffeic acid phenethyl ester (CAPE), an inhibitor of NF-κB activation, was used as a reference compound.[59,60].

$$\text{Inhibition } (\%) = (A - B)/(A - C) \times 100$$

A–*C*: nitrite concentration (μM);
A: LPS (+), Sample (−); *B*: LPS (+), Sample (+); *C*: LPS (−), Sample (−).

3.6.3. Determination of cytotoxic effects

Cytotoxicity was evaluated by the 3-(4,5-dimethyl-2-thiazolyl)-2,5-diphenyl-2*H*- tetrazolium bromide (MTT) colorimetric assay according to the previous reported conditions.[59] Briefly, RAW264.7 cells were cultured in DMEM, and the suspension of the cells were seeded into a 96-well microplate at 1.0×10^5 cells/200 μL/well. After 6 h, nonadherent cells were removed by washing with PBS, and the adherent cells were cultured in 100 μL of fresh medium containing the test compounds for 18 h. An aliquot of the medium (100 μL) was removed and MTT (10 μL, 5 mg/mL in PBS) solution was added. After a 2-h incubation at 37 °C, the medium was removed, and isopropanol containing 0.04 M HCl was added to dissolve the formazan produced in the cells. The optical density (OD) of the formazan solution was measured with a microplate reader at 570 nm (reference: 655 nm).

3.6.4. SDS–PAGE and Western blot analysis

RAW264.7 cells (5.0×10^6 cells/2 mL/well) were seeded into a 6-well multiplate and allowed to adhere for 6 h at 37 °C in a humidified atmosphere containing 5% CO_2. The cells were then washed with PBS, 1 mL of DMEM containing various concentrations of the

samples was added to each well, and after incubation for 10 min, 1 mL of DMEM containing LPS was added to stimulate the cells for 30 min or 12 h (final concentration of LPS, 10 μg/mL). The adhered cells were collected using a cell scraper in a lysis buffer (15 mM NaCl, 1 mM Tris, 1% Triton-X, 0.2 mM EGTA, 2.8 mM β-glycerophosphate) containing protease inhibitor cocktail (Thermo Scientific) and phosphatase inhibitor cocktail (PhosSTOP, Roche). Then, cells were disrupted three times (Microson™ ultrasonic cell disruptor, USA) for 30 s, and centrifuged at 10,000 rpm for 10 min. Protein concentrations of cell lysates were determined using the BCA™ protein assay kit. For protein sample preparation; 100 μL of supernatant was transferred to 50 μL of a dissolving agent (0.9 mM EGTA, 200 mM SDS, 2.8 mM Tris, 8% glycerol, 0.03% bromophenol blue, 6% mercaptoethanol). Then, the samples were heated in boiling water for 5 min. After cooling down, the samples were kept at −80 °C until used.[58,59]

Nuclear protein fraction was extracted 30 min after the stimulation with LPS using Nuclear and Cytoplasmic Extraction Reagent (Thermo Scientific) according to the manufacturer's instructions. The nuclear protein solution was concentrated using a Centrifugal Filter Units (Millipore Co., Ltd.) and applied for the electrophoresis.

Equivalent amounts of protein (50 μg of protein/lane for iNOS and β-actin, 25 μg of protein/lane for others) were electrophoresed in 10% SDS–polyacrylamide gels (Bio-Rad ready gel J) and transferred onto a polyvinylidene difluoride (PVDF) membranes (Bio-Rad, HC, USA). The membrane was then soaked in Tris-buffered saline containing 0.1% Tween 20 (T-TBS) with gentle shaking for 10 min, three times. For the blocking of the nonspecific sites, the membrane was soaked in Blocking One-P (for phosphorylated proteins: p-ERK1/2, p-JNK, p-p38, p-STAT1; Nacalai Tesque, Japan) or Blocking One (for others: iNOS, ERK1/2, JNK, p38, NF-κB, β-actin) by shaking for 0.5 h. The membrane was rinsed with T-TBS and incubated with specific primary antibodies: p-ERK1/2, ERK1/2, JNK1/2, p38, p-p38, NF-κB p65, STAT1, p-STAT1 (Ser 727), iNOS and β-actin (1:1000, Cell Signaling Technology). After incubation for 1 h at rt, the membrane was rinsed in T-TBS, and incubated in secondary antibodies (HRP-conjugated goat anti-mouse and anti-rabbit IgG, 1:5000) in an immunoreaction enhancer solution (Can Get Signal, Toyobo, Japan) for 1 h. Next, the membrane was shaken in T-TBS for 10 min, three times. The proteins were detected using an enhanced chemiluminescence (ECL) plus Western blotting detection system (Amersham™ GE Healthcare, Biosciences). The images of membranes were recorded using a luminescent image analyzer LAS-4000 mini (Fuji film, Japan). In our preliminary experiments, the amount of iNOS protein markedly increased 6 h after the treatment with LPS and remained higher after 24 h, and levels of p-ERK, p-JNK, p-p38, and p-STAT1 increased after 10 or 30 min and remained high for several hours (data not shown). Therefore, the effects of test compounds on iNOS protein levels were determined 12 h after the stimulation, and on other protein levels were determined 0.5 h after the stimulation.

3.7. Statistical analysis

All data are expressed as means ± SEM. The data analysis was performed with an one-way analysis of variance (1-ANOVA), followed by Dunnett's test. Probability (p) value of less than 0.05 was considered to be significant.

Acknowledgments

This work was supported by a Grant-in Aid for Scientific Research by the Japan Society for the Promotion of Science (JSPS).

References and notes

1. Poobrasert, O.; Constant, H. L.; Beecher, C. W. W.; Farnsworth, N. R.; Kinghorn, A. D.; Pezzuto, J. M.; Cordell, G. A.; Santisuk, T.; Reutrakul, V. *Phytochemistry* **1998**, *47*, 1661.
2. Mahidol, C.; Kaweetripob, W.; Prawat, H.; Ruchirawat, S. *J. Nat. Prod.* **2002**, *65*, 757.
3. Subhadhirasakul, S.; Pechpongs, P. *Songklanakarin J. Sci. Technol.* **2005**, *27*(Suppl. 2), 555.
4. Laphookhieo, S.; Maneerat, W.; Kiattansakul, R. *Can. J. Chem.* **2006**, *84*, 1546.
5. Prachyawarakorn, V.; Mahidol, C.; Ruchirawat, S. *Phytochemistry* **2006**, *67*, 924.
6. Laphookhieo, S.; Promnart, P.; Syers, J. K.; Kanjana-Opas, A.; Ponglimanont, C.; Karalai, C. *J. Braz. Chem. Soc.* **2007**, *18*, 1077.
7. Ngo, N. T. N.; Nguyen, V. T.; Vo, H. V.; Vang, O.; Duus, F.; Ho, T.-D. H.; Pham, H. D.; Nguyen, L.-H. D. *Chem. Pharm. Bull.* **2010**, *58*, 1487.
8. Kaweetripob, W.; Mahidol, C.; Prawat, H.; Ruchirawat, S. *Pharm. Biol.* **2000**, *38*(Suppl.), 55.
9. Mahidol, C.; Prawat, H.; Kaweetripob, W.; Ruchirawat, S. *Nat. Prod. Commun.* **2007**, *2*, 557.
10. Morikawa, T.; Xu, F.; Matsuda, H.; Yoshikawa, M. *Chem. Pharm. Bull.* **2006**, *54*, 1530.
11. Yoshikawa, M.; Xu, F.; Morikawa, T.; Pongpiriyadacha, Y.; Nakamura, S.; Asao, Y.; Kumahara, A.; Matsuda, H. *Chem. Pharm. Bull.* **2007**, *55*, 308.
12. Matsuda, H.; Ninomiya, K.; Morikawa, T.; Yasuda, D.; Yamaguchi, I.; Yoshikawa, M. *Bioorg. Med. Chem. Lett.* **2008**, *18*, 2038.
13. Yoshikawa, M.; Morikawa, T.; Funakoshi, K.; Ochi, M.; Pongpiriyadacha, Y.; Matsuda, H. *Heterocycles* **2008**, *75*, 1639.
14. Morikawa, T.; Funakoshi, K.; Ninomiya, K.; Yasuda, D.; Miyagawa, K.; Matsuda, H.; Yoshikawa, M. *Chem. Pharm. Bull.* **2008**, *56*, 956.
15. Morikawa, T.; Xie, Y.; Asao, Y.; Okamoto, M.; Yamashita, C.; Muraoka, O.; Matsuda, H.; Pongpiriyadacha, Y.; Yuan, D.; Yoshikawa, M. *Phytochemistry* **2009**, *70*, 1166.
16. Asao, Y.; Morikawa, T.; Xie, Y.; Okamoto, M.; Hamao, M.; Matsuda, H.; Muraoka, O.; Yuan, D.; Yoshikawa, M. *Chem. Pharm. Bull.* **2009**, *57*, 198.
17. Matsuda, H.; Ninomiya, K.; Morikawa, T.; Yasuda, D.; Yamaguchi, I.; Yoshikawa, M. *Bioorg. Med. Chem.* **2009**, *17*, 7313.
18. Morikawa, T.; Yamaguchi, I.; Matsuda, H.; Yoshikawa, M. *Chem. Pharm. Bull.* **2009**, *57*, 1292.
19. Muraoka, O.; Morikawa, T.; Miyake, S.; Akaki, J.; Ninomiya, K.; Yoshikawa, M. J. *Pharm. Biomed. Anal.* **2010**, *52*, 770.
20. Morikawa, T. *Yakugaku Zasshi* **2010**, *130*, 785.
21. Morikawa, T.; Xie, Y.; Ninomiya, K.; Okamoto, M.; Muraoka, O.; Yuan, D.; Yoshikawa, M.; Hayakawa, T. *Chem. Pharm. Bull.* **2010**, *58*, 1276.
22. Muraoka, O.; Morikawa, T.; Miyake, S.; Akaki, J.; Ninomiya, K.; Pongpiriyadacha, Y.; Yoshikawa, M. *J. Nat. Med.* **2011**, *65*, 142.
23. Xie, W.; Tanabe, G.; Akaki, J.; Morikawa, T.; Ninomiya, K.; Minematsu, T.; Yoshikawa, M.; Wu, X.; Muraoka, O. *Bioorg. Med. Chem.* **2011**, *19*, 2015.
24. Chaipech, S.; Morikawa, T.; Ninomiya, K.; Yoshikawa, M.; Pongpiriyadacha, Y.; Hayakawa, T.; Muraoka, O. *Chem. Pharm. Bull.* **2012**, *60*, 62.
25. Morikawa, T.; Chaipech, S.; Matsuda, H.; Hamao, M.; Umeda, Y.; Sato, H.; Tamura, H.; Kon'i, H.; Ninomiya, K.; Yoshikawa, M.; Pongpiriyadacha, Y.; Hayakawa, T.; Muraoka, O. *Bioorg. Med. Chem.* **2012**, *20*, 832.
26. Chaipech, S.; Morikawa, T.; Ninomiya, K.; Yoshikawa, M.; Pongpiriyadacha, Y.; Hayakawa, T.; Muraoka, O. J. *Nat. Med.* **2012**, *66*, 486.
27. Morikawa, T.; Chaipech, S.; Matsuda, H.; Hamao, M.; Umeda, Y.; Sato, H.; Tamura, H.; Ninomiya, K.; Yoshikawa, M.; Pongpiriyadacha, Y.; Hayakawa, T.; Muraoka, O. J. *Nat. Med.* **2012**, *66*, 516.
28. Joshi, B. S.; Kamat, V. N.; Govindachari, T. R.; Ganguly, A. K. *Tetrahedron* **1969**, *25*, 1453.
29. Crombie, L.; Games, D. E.; Haskins, N. J.; Read, G. F. *Tetrahedron Lett.* **1970**, *3*, 251.
30. Deng, Y.; Nicholson, R. A. *Planta Med.* **2005**, *71*, 364.
31. Verotta, L.; Lovaglio, E.; Vidari, G.; Finzi, P. V.; Neri, M. G.; Raimondi, A.; Parapini, S.; Taramelli, D.; Riva, A.; Bombardelli, E. *Phytochemistry* **2004**, *65*, 2867.
32. Yagi, N.; Ohkubo, K.; Okuno, Y.; Oda, Y.; Miyazawa, M. *J. Oleo Sci.* **2006**, *55*, 173.
33. Win, N. N.; Awale, S.; Esumi, H.; Tezuka, Y.; Kadota, S. *Bioorg. Med. Chem. Lett.* **2008**, *18*, 4688.
34. Win, N. N.; Awale, S.; Esumi, H.; Tezuka, Y.; Kadota, S. *Bioorg. Med. Chem.* **2008**, *16*, 8653.
35. Thebtaranonth, C.; Imraporn, S.; Padungkul, N. *Phytochemistry* **1981**, *20*, 2305.
36. Morel, C.; Guilet, D.; Oger, J.-M.; Séraphin, D.; Sévenet, T.; Wiart, C.; Hadi, A. H. A.; Richomme, P.; Bruneton, J. *Phytochemistry* **1999**, *50*, 1243.
37. Crombie, L.; Jones, R. C. F.; Palmer, C. J. *J. Chem. Soc., Perkin Trans. 1* **1987**, 317.
38. Cruz, F. G.; da Silva-Neto, J. T.; Guedes, M. L. S. *J. Braz. Chem. Soc.* **2001**, *12*, 117.
39. Yang, H.; Protiva, P.; Gil, R. R.; Jiang, B.; Baggett, S.; Basile, M. J.; Reynertson, K. A.; Weinstein, I. B.; Kennelly, E. J. *Planta Med.* **2005**, *71*, 852.
40. β-Amyrin and benzoic acid were identified by comparison of their physical data with those of commercially obtained samples.
41. The ^{1}H and ^{13}C NMR spectra of **1** and **2** were assigned with the aid of distortionless enhancement by polarization transfer (DEPT), 1H–1H correlation spectroscopy (^{1}H–^{1}H COSY), heteronuclear multiple quantum coherence (HMQC), and heteronuclear multiple bond correlation spectroscopy (HMBC) experiments.

42. Ohtani, I.; Kusumi, T.; Kashman, Y.; Kakisawa, H. J. *Am. Chem. Soc.* **1991**, *113*, 4092.
43. Kontush, A.; Chapman, M. J. *Pharmcol. Rev.* **2006**, *58*, 342.
44. Hansson, G. K. *New Eng. J. Med.* **2005**, *352*, 1685.
45. MacMicking, J.; Xie, Q. W.; Nathan, C. *Ann. Rev. Immunol.* **1997**, *15*, 323.
46. Rao, Y. K.; Fang, S. H.; Tzeng, Y. M. *J. Ethnopharmacol.* **2005**, *100*, 249.
47. Qu, D. M.; Zheng, Y. G. *Pathophysiol. Clin. Med.* **1997**, *17*, 270.
48. Luo, Y.; Wu, K.; Sun, A.; Pan, B.; Zhang, X.; Fan, D. *Chin. J. Digest. Dis.* **2001**, *2*, 120.
49. Bogdan, C. *Nat. Immunol.* **2001**, *2*, 907.
50. Kumar, A. P.; Ryan, C.; Cordy, V.; Reynolds, W. F. *Nitric Oxide* **2005**, *13*, 2.
51. Zang, M. W.; Liu, J. S. *Pathophysiol. Clin. Med.* **1998**, *18*, 37.
52. Matsuda, H.; Ando, S.; Kato, T.; Morikawa, T.; Yoshikawa, M. *Bioorg. Med. Chem.* **2006**, *14*, 138.
53. Yoshikawa, M.; Nishida, N.; Ninomiya, K.; Ohgushi, T.; Kubo, M.; Morikawa, T.; Matsuda, H. *Bioorg. Med. Chem.* **2006**, *14*, 456.
54. Morikawa, T.; Abdel-Halim, O. B.; Matsuda, H.; Ando, S.; Muraoka, O.; Yoshikawa, M. *Tetrahedron* **2006**, *62*, 6435.
55. Morikawa, T. *J. Nat. Med.* **2007**, *61*, 112.
56. Yoshikawa, M.; Morikawa, T.; Oominami, H.; Matsuda, H. *Chem. Pharm. Bull.* **2009**, *57*, 957.
57. Morikawa, T.; Oominami, H.; Matsuda, H.; Yoshikawa, M. *J. Nat. Med.* **2011**, *65*, 129.
58. Sae-Wong, C.; Matsuda, H.; Tewtrakul, S.; Tansakul, P.; Nakamura, S.; Nomura, Y.; Yoshikawa, M. *J. Ethnopharmacol.* **2011**, *136*, 488.
59. Hegazy, M. E.; Matsuda, H.; Nakamura, S.; Yabe, M.; Matsumoto, T.; Yoshikawa, M. *Chem. Pharm. Bull.* **2012**, *60*, 363.
60. Natarajan, K.; Singh, S.; Burke, T. R., Jr.; Grunber-ger, D.; Aggarwal, B. B. *Proc. Natl. Acad. Sci. U.S.A.* **1996**, *93*, 9090.
61. Kieran, M. W.; Zon, L. I. *Curr. Opin. Hematol.* **1996**, *3*, 27.
62. Kurosawa, M.; Numazawa, S.; Tani, Y.; Yoshida, T. *Am. J. Physiol. Cell Physiol.* **2000**, *278*, 500.
63. Moon, D. O.; Park, S. Y.; Lee, K. J.; Heo, M. S.; Kim, K. C.; Kim, M. O.; Lee, J. D.; Choi, Y. H.; Kim, G. Y. *Int. Immunopharmacol.* **2007**, *7*, 1092.
64. Park, H. J.; Lee, H. J.; Choi, M. S.; Son, D. J.; Song, H. S.; Song, M. J.; Lee, J. M.; Han, S. B.; Kim, Y.; Hong, J. T. *J. Inflamm. (Lond.)* **2008**, *5*, 7.
65. Lin, H. T.; Shen, S. C.; Lin, C. W.; Wu, M. S.; Chen, Y. C. *Chem. Biol. Interact.* **2009**, *180*, 202.
66. Hwang, J. M.; Yu, J. Y.; Jang, Y. O.; Kim, B. T.; Hwang, K. J.; Jeon, Y. M.; Lee, J. C. *Int. Immunopharmacol.* **2010**, *10*, 526.
67. Kawai, T.; Takeuchi, O.; Fujita, T.; Inoue, J.; Muhlradt, P. F.; Sato, S.; Hoshino, K.; Akira, S. *J. Immunol.* **2001**, *167*, 5887.
68. Ando, S.; Matsuda, H.; Morikawa, T.; Yoshikawa, M. *Bioorg. Med. Chem.* **2005**, *13*, 3289.
69. Shen, T.; Park, Y. C.; Kim, S. H.; Lee, J.; Cho, J. Y. *Biol. Pharm. Bull.* **2010**, *33*, 1159.

Journal of Pharmaceutical and Biomedical Analysis 70 (2012) 718–726

Contents lists available at SciVerse ScienceDirect

Journal of Pharmaceutical and Biomedical Analysis

journal homepage: www.elsevier.com/locate/jpba

Comparative studies on glycoproteins expressing polylactosamine-type N-glycans in cancer cells

Yosuke Mitsui [a], Keita Yamada [a], Sayaka Hara [a], Mitsuhiro Kinoshita [a], Takao Hayakawa [b], Kazuaki Kakehi [a,*]

[a] School of Pharmacy, Kinki University, Kowakae 3-4-1, Higashi-Osaka 577-8502, Japan
[b] Pharmaceutical Research and Technology Institute, Kinki University, Kowakae 3-4-1, Higashi-Osaka 577-8502, Japan

ARTICLE INFO

Article history:
Received 8 March 2012
Received in revised form 21 June 2012
Accepted 25 June 2012
Available online 4 July 2012

Keywords:
Cancer-specific glycoproteins
N-glycans
LC–MS
Lectin affinity chromatography
Western blot

ABSTRACT

In the series of our previous reports, we showed that some cancer cell lines specifically express polylactosamine-type N-glycans and such glycans were often modified with fucose and sulfate residues. To confirm the proteins expressing these glycans, glycopeptide mixture obtained by digestion of whole protein fractions with trypsin was captured by a polylactosamine-specific lectin, *Datura strasmonium* agglutinin (DSA). And the peptides and glycans of the captured glycopeptides after digestion with N-glycoamidase F were extensively analyzed by HPLC and MS techniques. We found that some glycoproteins such as CD107a and CD107b commonly contained polylactosamine-type glycans in all the examined cancer cells. But integrin-α5 (CD49e) and carcinoembryonic antigen-related cell adhesion molecule 5 (CD66e) having these glycans were specifically found in U937 (human T-lymphoma) and MKN45 (human gastric cancer) cells, respectively. These data clearly indicate that specific glycans attached to specific proteins will be promising markers for specific tumors with high accuracy.

1. Introduction

Glycans in glycoconjugates such as glycoproteins, proteoglycans and glycolipids participate in various biological events such as cell recognition, cell–cell interaction, inflammation, and disease progression [1,2]. Aberrant glycosylation has been known to be associated with various human diseases, particularly with tumors. And a number of clinical cancer biomarkers are often glycoproteins such as carcinoembryonic antigen (CEA; CD66) as a marker of colorectal cancer, cancer antigen 125 (CA-125) for diagnosis of ovarian cancer and prostate-specific antigen (PSA).

Biosynthesis of the glycans in glycoproteins is regulated by a number of factors such as (a) expression of related glycosyltransferases and/or glycosidases, (b) proper locations, and (c) the functional machinery of sugar nucleotides. Thus, micro environmental changes in the synthesis of glycans greatly affect their synthetic efficiency and also their structures. For example, complex-type N-glycans having polylactosamine-type structures are predominantly present when cells are tumorized. However, it has been challenging to analyze specific glycans in comprehensive and quantitative manner, because extremely a minute amount of glycans are available in biological samples.

In our previous papers, we proposed a series of methods for the analysis of glycans of glycoproteins in biological samples [3–5]. The methods include several separation/analysis steps. Initially, total glycan pool obtained from biological samples such as cell membrane fractions by enzymatic/chemical methods was fluorescently labeled with 2-aminobenzoic acid (2AA), and separated based on the number of sialic acid residues attached to the glycans using affinity chromatography on a serotonin-immobilized stationary phase. In this step, we can determine total amounts of glycans as well as those of each category of glycans (asialo/high-mannose, mono-, di-, tri- and tetra-sialoglycans). Then, the collected glycan groups were analyzed by LC/MS^n technique. Capillary affinity electrophoresis and digestion with specific exoglycosidases for linkage analysis were also employed. Based on the studies using these techniques, we found that U937 cells (histiocytic lymphoma cells), ACHN cells (human kidney glandular cancer cells), MKN45 cells (human gastric cancer cells), A549 cells (human lung cancer cells), and Jurkat cells (acute T-cell leukemia) express a large amount of N-glycans having polylactosamine residues.

There are a number of reports regarding the functions and distributions of polylactosamine-type glycans [6]. And the proteins to which polylactosamine-type glycans are attached were also reported by Fukuda et al. [7]. They employed *Datura stramonium* agglutinin (DSA) affinity chromatography for capturing proteins carrying polylactosamine-type glycans [8]. Togayachi et al. reported that polylactosamine residues on glycoproteins influenced basal levels of lymphocyte and macrophage activation.

* Corresponding author. Tel.: +81 6 6721 2332; fax: +81 6 6721 2353.
E-mail address: k_kakehi@phar.kindai.ac.jp (K. Kakehi).

0731-7085/$ – see front matter © 2012 Elsevier B.V. All rights reserved.
http://dx.doi.org/10.1016/j.jpba.2012.06.035

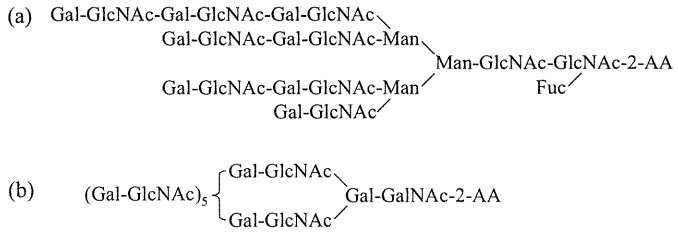

Fig. 1. Typical structures of polylactosamine-type glycans. (a) N-glycans and (b) O-glycans.

They employed *Lycopersicon esculentum* (tomato) agglutinin (LEA), which recognizes the repeats of polylactosamine units [9].

In our previous report on the analysis of N-glycans in cancer cells, we found that lactosamine units were elongated at all the branches of tri- and tetra-antennary glycans (Fig. 1a) [3]. In contrast, they form a long chain of polylactosamine-units in mucin-type O-glycans (Fig. 1b) [4].

This is probably due to branching effect of N-glycans which accerelate the addition of lactosamine residues to every branches of the glycans. We need to clarify the reasons why polylactosamine-glycans are elongated in different manners in Asn-linked N-glycans and mucin-type O-glycans in order to understand glycan profiles for clinical use.

In the present study, we attempted to confirm glycoprotein(s) which express polylactosamine-type N-glycans in several cancer cell lines. In addition, polylactosamine-carrying glycoproteins are compared among several cancer cell lines. And we propose that comparative studies of the proteins which express specific glycans on various cancer cell lines afford important information on diagnosis for cancer stages.

2. Materials and methods

2.1. Materials

Enzyme. Peptide N-glycoamidase F (EC 3.5.1.52) was obtained from Roche Diagnostics (Mannheim, Germany). Neuraminidase (*Arthrobacter ureafaciens*) was kindly donated by Dr. Ohta (Marukin-Bio, Uji, Kyoto, Japan). Benzonase was obtained from Novagen (Darmstadt, Germany). TPCK-treated trypsin was from Worthington (Lakewood, NJ). *Antibody.* LAMP-1 (H4B3) mouse IgG_1 monoclonal, LAMP-2 (H4B4) mouse IgG_1 monoclonal and integrin α5 (D-9) mouse IgG_{2a} monoclonal were from Santa Cruz Biotechnology (Santa Cruz, CA). Basigin (MEM-M6/1) mouse IgG_1 monoclonal was from Abcam (Cambridge, UK). Transferrin receptor mouse IgG_1 monoclonal was kindly donated by Dr. Yagi (Kinki University, School of Pharmacy). *Chemicals.* 2-Iodoacetamide was from Tokyo Kasei (Chuo-ku, Tokyo, Japan). Dithiothreitol (DTT) was obtained from Nacalai Tesque (Nakagyo-ku, Kyoto, Japan). 3,3′-Diaminobenzidine, tetrahydrochloride (DAB) was obtained from DOJINDO (Kamimashiki-gun, Kumamoto, Japan). 2-Aminobenzoic acid (2AA) and sodium cyanoborohydride for fluorescent labeling of oligosaccharides were from Tokyo Kasei. Coomassie brilliant blue G-250 was purchased from Bio-Rad (Hercules, CA). Sephadex LH-20 was from Amerscham Bioscience (Upsala, Sweden). Vivaspin 500 was obtained from Sartorius (Goettingen, Germany). DSA-agarose and DSA-biotin were obtained from Seikagaku Kogyo (Chuoku, Tokyo, Japan). LEA-agarose and VECTA Elite ABC mouse IgG kit for Western blotting were obtained from Vector Labs (Burlingame, CA). Immobilon-P Transfer Membrane (PVDF) was obtained from Millipore (Bedford, MA). Protein inhibitor cocktail for animal cells was obtained from Nacalai Tesque. Protein G Sepharose 4 Fast Flow was obtained from GE Healthcare (Upsala, Sweden). All other reagents and solvents were of the highest grade commercially available or of HPLC grade. All aqueous solutions were prepared using water purified with a Milli-Q purification system (Millipore, Bedford, MA).

2.2. Cell culture

In the present study, we used the following cell lines: U937 cells (human T-lymphoma cells), ACHN cells (human kidney glandular cancer cells), MKN45 cells (human gastric cancer cells), A549 cells (human lung cancer cells), and Jurkat cells (acute T cell leukemia). The cells except for A549 were cultured in RPMI-1640 medium supplemented with 10% (v/v) fetal calf serum and 1% (v/v) penicillin–streptomycin solution (10,000 U penicillin and 10 mg streptomycin/mL; Nacalai Tesque). A549 cells were cultured in Dulbecco's modified Eagle's medium supplemented with 10% (v/v) fetal calf serum and 1% (v/v) penicillin–streptomycin solution. Fetal calf serum was previously kept at 56 °C for 30 min. The cells were cultured at 37 °C under 5% CO_2 atmosphere, and harvested at 80% confluent state. Cells (1×10^7 cells) were washed with phosphate buffered saline (PBS), and collected by centrifugation at 1000 rpm for 20 min.

2.3. Extraction of whole proteins from cancer cells and digestion with trypsin

Cancer cells (1.0×10^7 cells) were suspended in PBS containing 1 mM EDTA (50 μL), and kept at room temperature for 15 min. Extraction reagent (7 M urea, 2 M thiourea, 4% CHAPS, 30 mM Tris–HCl (pH 8.5, 268 μL)), 1 M DTT (17 μL) and benzonase (125 units, 5 μL) were added to the suspended cells. After 30 min, the mixture was centrifuged at 8000 × *g* for 15 min. The supernatant layer was collected and boiled for 5 min at 100 °C, and evaporated to dryness by a centrifugal evaporator (Speed Vac, Servant, Sunnydale, CA). Guanidine solution (2 mM EDTA, 0.5 M Tris–HCl and 4 M guanidine (pH 8.5, 80 μL)) was added to the lyophilized material. After dissolution of the lyophilized material, 0.18 M DTT in guanidine solution (40 μL) was added to the mixture. The mixture was kept at 37 °C for 90 min. After addition of 0.18 M iodoacetamide in guanidine solution (155 μL), the mixture was kept for 45 min in a dark place. After addition of acetone solution (85% acetone, 5% triethylamine, 5% acetic acid in water (1.7 mL)), the mixture was kept at −20 °C for 30 min, and the precipitate was collected by centrifugation at 8000 × *g* for 15 min and washed with 75% ethanol (1 mL × 2). The precipitate was evaporated to dryness by a centrifugal evaporator. The dried material was digested with trypsin (100 μg) in 2 M urea, 0.1 M Tris–HCl (pH 8.6, 800 μL) at 37 °C overnight. After the reaction, the mixture was boiled for 10 min, and the supernatant was collected, and passed through an ultrafiltration membrane (MW cut off, 5000 Da). The residual solution on the membrane was used as a mixture of glycopeptides.

2.4. Collection of glycopeptides having polylactosamine-type glycans by lectin affinity chromatography using a DSA-immobilized agarose column, and digestion of the captured glycopeptides with N-glycoamidase F

The solution of the glycopeptide mixture obtained as described above was applied to a DSA-immobilized column (DSA 3.8 mg (7.9 nmol)/1 mL of agarose) which had been previously equilibrated with PBS. Unbound peptides were eluted with 15 mL of PBS. Then, bound glycopeptides were eluted with 0.1 M N-acetyl D-glucosamine in PBS (15 mL). The bound and unbound fractions were passed through an ultrafiltration membrane (MW cut off, 3000 Da), respectively, and the residual solution on the membrane was evaporated to dryness by a centrifugal evaporator. The dried materials were digested with N-glycoamidase F (2 units, 2 μL) in

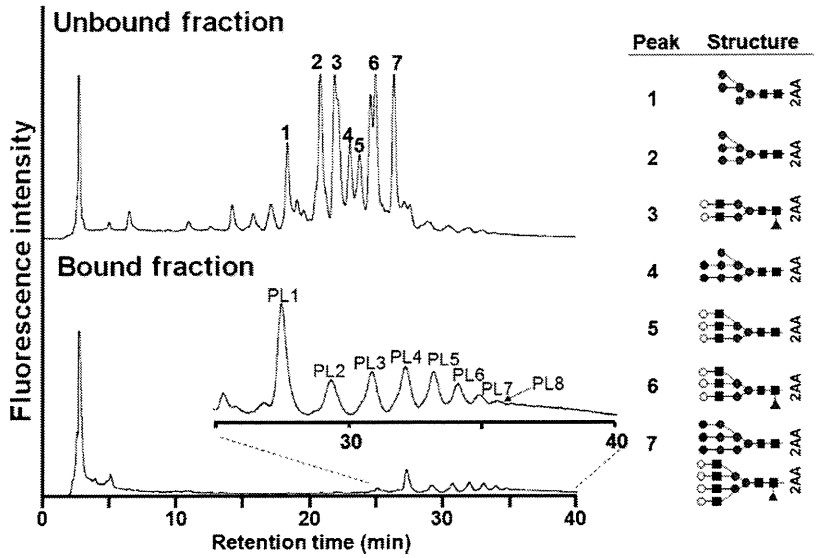

Fig. 2. HPLC analysis of the peaks observed in DSA-bound fractions. The N-glycans were previously digested with neuraminidase. Analytical conditions: column, TSK-Gel Amide-80 (4.6 mm × 250 mm); eluent: A, 0.2% acetic acid/acetonitrile; B, 0.5% acetic acid–0.3% triethylamine/water. Gradient elution, 0–2 min (30% solvent B), 2–82 min (30–95% solvent B), 82–102 min (95% solvent B). Detection, Ex 350 nm, Em 425 nm. Column temp. 40 °C.

100 mM phosphate buffer (pH 7.5, 100 μL) at 37 °C overnight. After keeping the enzyme reaction mixture in the boiling water bath for 10 min, the mixture was centrifuged at 8000 × *g* for 10 min. The supernatant solutions were collected and lyophilized to dryness.

2.5. Fluorescent labeling of the released N-glycans with 2-aminobenzoic acid (2AA) and analysis of the labeled glycans by HPLC

A portion (1.2×10^7 cells) of the dried material obtained by digestion with N-glycoamidase F (see Section 2.4) was dissolved in 2AA solution (100 μL) which was freshly prepared by dissolution of 2AA (30 mg) and sodium cyanoborohydride (30 mg) in methanol (1 mL) containing 4% sodium acetate and 2% boric acid. The mixture was kept at 80 °C for 1 h. After cooling, water (100 μL) was added to the mixture, and applied to a column of Sephadex LH-20 (1.0 cm i.d., 30 cm length) equilibrated with 50% aqueous methanol. Fluorescent intensities of each fraction were monitored at 410 nm irradiated with a 335-nm light. The earlier eluted fluorescent fractions were pooled and evaporated to dryness under reduced pressure. The lyophilized materials were digested with neuraminidase (2 munits, 4 μL) in 20 mM acetate buffer (pH 5.0, 100 μL) at 37 °C overnight. After keeping the mixture in the boiling water bath for 10 min, the mixture was centrifuged at 8000 × *g* for 10 min. The supernatant solution was collected and lyophilized to dryness, and the dried materials were dissolved in water. And a portion (5×10^6 cells; 3 μL) was analyzed by a Jasco HPLC apparatus equipped with two PU-980 pumps and a Jasco FP-920 fluorescence detector (Hachio-ji, Tokyo, Japan). Separation was done with an Amide-80 column (Tosoh, 4.6 × 250 mm) using a linear gradient formed by 0.2% acetic acid in acetonitrile (solvent A) and 0.5% acetic acid in water containing 0.3% triethylamine (solvent B). The column was initially equilibrated and eluted with 70% solvent A for 2 min, from which point solvent B was increased to 95% over 80 min, and kept at this composition for further 100 min. Flow rate was kept at 1.0 mL/min. The observed peaks were collected and lyophilized to dryness for the analysis by matrix-assisted laser-desorption ionization time-of-flight (MALDI-TOF) mass spectrometry.

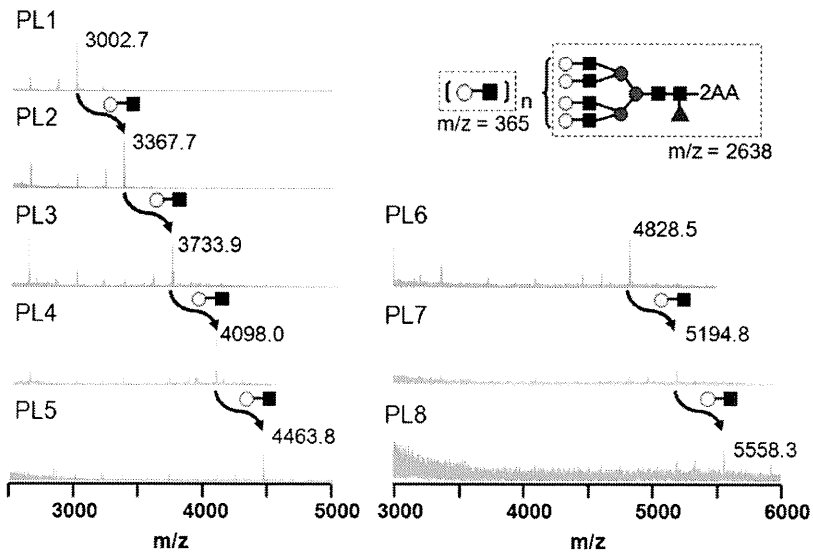

Fig. 3. MS analysis of the peaks observed in Fig. 2.

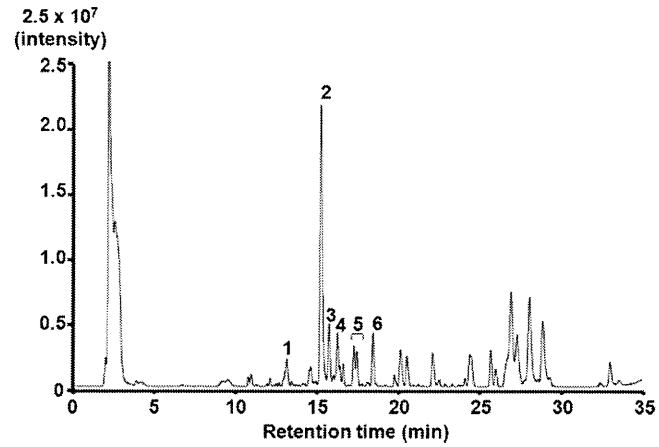

Fig. 4. Total ion chromatogram of DSA-bound glycopeptides. Analytical conditions: see Section 2.

2.6. MALDI-TOF MS analysis

MALDI-TOF MS spectra of 2AA-labeled glycans were acquired on a MALDI-QIT TOF mass spectrometer (AXIMA-QIT, Shimadzu, Kyoto, Japan). Acquisition and data processing were controlled by a Launchpad software (Kratos Analytical, Manchester, UK). Typically, a 0.5-μL portion of the matrix solution (DHB; 10 mg/mL in 30% ethanol/0.1% trifluoroacetic acid) was deposited on the stainless steel target plate and allowed to dry. Then, a portion (0.5 μL) of the appropriately diluted analyte solution (typically ca. 1 pmol/μL) was used to cover the matrix on the target plate and allowed to dry at room temperature.

2.7. Liquid chromatography (LC) ion-trap time-of-flight (IT-TOF) MS analysis of peptides

Positive electrospray ionization (ESI)-MS analyses were conducted with an LC–IT-TOF MS instrument (Shimadzu, Kyoto) connected with an HPLC system (LC-20AD pump, CTO-20AC column oven, and CBM-20A system controller; Shimadzu, Kyoto). A portion (5×10^6 cells; 3 μL) of the aqueous solution of the peptide mixture obtained after digestion with N-glycoamidase F (see Section 2.4) was injected to a reverse-phase column (HiQ sil C_{18V} column, 2.1 mm × 150 mm; KYA TECH), and analyzed using the following gradient program. Solvent A was 5% acetonitrile/0.1% formic acid. Solvent B was 95% acetonitrile/0.1% formic acid. The column was initially equilibrated and eluted with 95% solvent A for 5 min, from which point solvent B was increased to 75% over 30 min at a flow rate of 0.2 mL/min. Column temperature was kept at 40 °C. The MS apparatus was operated at a probe voltage of 4.50 kV, CDL temperature of 200 °C, block heater temperature of 200 °C, nebulizer gas flow of 1.5 L/min, ion accumulation time of 30 ms. MS range was from *m/z* 200 to 2000, and MS/MS range also from *m/z* 200 to 2000. CID parameters were as follows: energy, 50%; collision gas, 50%. Monoisotopic ion was used as the precursor ion. MS data were processed with LCMS solution ver. 3.6 software (Shimadzu).

2.8. Peptides mass finger printing

For protein identification, Mascot generic format (MGF) files generated from MS/MS spectra were uploaded to MASCOT search (Matrix Science, London, UK: http://www.matrixscience.com). The parameters for database search were as follows: protein database was set to Swiss PROT. Taxonomy was set to homo sapience. One trypsin missed cleavage was allowed. The mass tolerance was set to 0.5 Da for precursor ions and 0.6 Da for product ions. Carbamidomethyl (C) was chosen as a fixed modification. Deamidation (NQ) was chosen for variable modifications. Data format was chosen as Mascot generic, and instrument was chosen as ESI-TRAP-TOF.

2.9. Sodium dodecyl sulfate-polyacrylamide gel electrophoresis (SDS-PAGE)

After addition of SDS-PAGE sample buffer (250 mM Tris–HCl (pH 6.8)–4.6% SDS, 20% glycerol), 2-mercaptoethanol and water (10:9:1, 2 mL) to the cell pellet (2×10^7 cell), the mixture was vortexed, and boiled for 10 min. The supernatant was collected after centrifugation and used for SDS-PAGE. SDS-PAGE was performed with a Mini protean 3 Cell and a POWER PAC 3000 (Bio-Rad, Hercules, CA). The amount of the applied protein was 25 μg/lane. Separation gel was 10%. Electrophoresis buffer was 25 mM Tris, 198 mM glycine, 1% (w/v) SDS in water.

After SDS-PAGE, the gel was stained with Coomassie brilliant blue G-250 (CBB) for 1 h. CBB solution contains 40% methanol, 10% acetic acid, and 0.2% Coomassie brilliant blue G-250. The gel was destained with 40% methanol–10% acetic acid.

2.10. Western blot

Western blot was performed with a semi-dry electrophoretic transfer cell (Trans-Blot SD, Bio-Rad, Hercules, CA). PVDF membrane was kept in methanol for 1 min and in the blotting buffer (48 mM Tris, 39 mM glycine and 20% methanol (pH9.0)) for 1 h. Cell lysate (25 μg as protein) of U937 cells was resolved using reducing 9% SDS-PAGE and transferred to a PVDF membrane. The membrane was incubated in blocking buffer (5% skim milk, 0.05% Tween 20 in PBS). After washing with 0.05% Tween 20/PBS (20 mL 4×), the membrane was reacted with primary antibody overnight. All the primary antibodies were used at the same concentration (5 μg/mL, 5 mL). After washing with 0.05% Tween 20/PBS (20 mL 4×), the membrane was reacted with biotin conjugated with secondary antibodies (5 μg/mL, 5 mL) for 1 h. After washing with 0.05% Tween 20/PBS (20 mL), the PVDF membrane was reacted with HRP labeled avidin (5 μg/mL, 5 mL in PBS) for 1 h. After washing with 0.05% Tween 20/PBS (20 mL 4×), the membrane was visualized with 0.05% DAB, 0.0031% hydrogen peroxide in 100 mM Tris–HCl buffer (pH 7.5).

2.11. Lectin blot

SDS-PAGE and electrophoretic transferring were performed in the same manner as described above. After the gel was transferred to a PVDF membrane, the membrane was incubated in 0.05% Tween 20 in PBS, and reacted with biotin-labeled DSA lectin (5 μg/mL, 5 mL) for 1 h. After washing the membrane with 0.05% Tween 20 in PBS (20 mL 4×), the membrane was reacted with HRP-labeled avidin (5 μg/mL, 5 mL) for 30 min. After washing with 0.05% Tween 20 in PBS (20 mL 4×), the membrane was visualized with 0.05% DAB, 0.0031% hydrogen peroxide in 100 mM Tris–HCl buffer (pH 7.5).

2.12. Immunoprecipitation of target proteins

Lysis buffer (20 mM HEPES, 150 mM NaCl, 1 mM EDTA, 1.0% Triton X-100, 0.5% deoxycholate, 0.1% SDS, 950 μL) and protease inhibitor (50 μL) were added to the pellet of U937 cells (2×10^7 cells). The mixture was vortexed for 10 min and incubated on an ice bath for 30 min, and centrifuged at 8000 × *g* for 30 min. The supernatant was collected, and used for immunoprecipitation.

Antibody for the specific protein (50 μg/mL, 100 μL) was added to Protein G Sepharose (100 μL), and the mixture was incubated for

Table 1
Glycoproteins identified in whole proteins of U937.

Peak no.	Proposed proteins	Peptide sequence	Precursor mass (*m/z*)	Score	Subcellular location
1	Integrin α5 (CD49e)	NL***NNS***QSDVVSFR	$[M+2H]^{2+}$ = 741.32	31	Membrane
2	Basigin (CD147)	ILLTCSL***NDS***ATEVTGHR	$[M+3H]^{3+}$ = 663.32	42	cell membrane, melanosome
3	Lysosome-associated membrane glycoprotein-1 (CD107a)	SSCGKE***NTS***DPSLVIAFGR	$[M+3H]^{3+}$ = 675.97	13	Cell membrane, endosome membrane, lysosome membrane
4	4F2 cell-surface antigen heavy chain (CD98)	SLVTQYL***NAT***GNR	$[M+2H]^{2+}$ = 719.35	69	Apical cell membrane, melanosome
	Sortilin	DITDLI***NNT***FIR	$[M+2H]^{2+}$ = 718.37	25	Cell membrane
5	Lysosome-associated membrane glycoprotein-1 (CD107a)	SGPK***NMT***FDLPSDATVVL***NR***	$[M+3H]^{3+}$ = 722.01	23	Cell membrane, endosome membrane, lysosome membrane
	Lysosome-associated membrane glycoprotein-2 (CD107b)	VASVININP***NTT***HSTGSCR	$[M+3H]^{3+}$ = 676.99	21	Cell membrane, endosome membrane, lysosome membrane
6	Transferrin receptor protein-1 (CD71)	DFEDLYTPV***NGS***IVIVR	$[M+2H]^{2+}$ = 969.47	12	Cell membrane, melanosome

1 h. Protein G Sepharose thus prepared was washed with PBS (1 mL 3×), and the protein mixture obtained from the cells (1×10^7 cells, see above) was added. The mixture was incubated at 4 °C overnight with gentle shaking. Protein G Sepharose was washed with PBS (1 mL 6×). After addition of SDS sample buffer (20 μL) and 2-mercaptoethanol (2 μL), Protein G Sepharose was boiled for 10 min. The supernatant was collected by centrifugation, and used for SDS-PAGE analysis.

2.13. In-gel digestion with N-glycoamidase F

Specific proteins collected by immunoprecipitation were analyzed by SDS-PAGE followed by staining with CBB. After changing the destaining solution with water, bands of specific proteins detected by Western blot were cut, and the gel pieces were destained with 30% acetonitrile (300 μL 2×) for 30 min and dehydrated with acetonitrile (200 μL 2×) for 10 min. After drying the gel pieces, the gel pieces were digested with N-glycoamidase F (2 units, 2 μL) in 100 mM phosphate buffer (pH 7.5, 100 μL) at 37 °C overnight. N-Glycans thus released were extracted with water (200 μL 3×) for 30 min, and the supernatant solution was lyophilized to dryness for labeling with 2AA.

3. Results and discussion

3.1. Identification of glycoproteins carrying polylactosamine-type N-glycans in U937 cells

Our group previously reported that U937 cells (histiocytic lymphoma cells) specifically expressed large amount of polylactosamine-type N-glycans [3]. As the initial study, we identified glycoproteins carrying polylactosamine-type N-glycans in U937 cells.

After whole proteins collected from U937 cells were digested with trypsin, DSA-immobilized and LEA-immobilized agarose columns were used for capturing polylactosamine-carrying peptides. The collected bound fractions from each of DSA and LEA immobilized columns were digested with N-glycoamidase F, and the released N-glycans were labeled with a fluorescent reagent, 2AA. Then, the mixture of the fluorescent labeled glycans were digested with neuraminidase, and analyzed by HPLC and MALDI-TOF MS. In the previous studies on the comprehensive analyses of N-glycans in various cancer cells, we found that lactosamine residues are attached to all the branches of tetraantennary glycans as shown in Fig. 1a [3]. DSA lectin preferentially recognizes tri- and tetra-antennary glycans [10]. On the other hand, LEA lectin binds to an elongated polylactosamine chain in glycans as indicated in Fig. 1b [9]. As shown in Fig. 2, characteristic ladder peaks (PL1–PL8) due to polylactosamine-type glycans were observed in DSA-bound fractions. In contrast, high-mannose, tri- and tetra-antennary glycans were observed abundantly in unbound fractions (the list of the structures in Fig. 2).

However, glycan peaks were not observed in LEA-bound fractions (data not shown). This means that lactosamine units are bound to the branches of tetraantennary glycans as indicated in Fig. 1a. The mass spectra of the peaks observed in the bound fractions are shown in Fig. 3.

The molecular ion at *m/z* 3002 (PL1) corresponds to the monofucosylated tetra-antennary glycan to which one lactosamine residue is attached. And the molecular ions increase by *m/z* 365 from PL1 to PL8. PL8 showing the largest molecular ion at *m/z* 5558 is the tetra-antennary glycan having eight polylactosamine residues. We already reported the structure of PL4 as shown in Fig. 1a [3]. From these results, polylactosamine-type glycans were selectively concentrated in the DSA-bound glycopeptides. It should be noticed that other glycans such as those having high-mannose type glycans were not included in the bound fractions. And this means that polylactosamine-type N-glycans preferentially attach to the specific peptide (see below).

Based on the analyses of the N-glycans, peptide portions of the DSA-bound glycopeptides which contained polylactosamine-type glycans were analyzed by LC–MS (Fig. 4).

More than 25 peaks were observed in the total ion chromatogram. The peaks observed from 13 min to 19 min showed higher molecular ions than *m/z* 1000. On the other hand, the peaks eluted later than 20 min showed low molecular ions (less than *m/z* 500). The small peptides of which molecular weights are less than *m/z* 500 have little information on amino acid sequences. Therefore, we analyzed the peaks showing large molecular ions by MS/MS, and identified that seven peaks were due to specific glycoproteins as shown in Table 1 by Mascot analysis.

Of the confirmed glycoproteins, integrin expressing multiantennary glycans was reported to play some functions on metastasis of tumors [11]. Lysosome-associated membrane glycoproteins (LAMP-1 and LAMP-2; peak 3 and peak 5) and basigin (peak 2) are glycoproteins having polylactosamine-type N-glycans [7,12,13]. CD98, transferrin receptor protein-1 as well as sortilin have N-glycans, although the presence of polylactosamine-type glycans was not clear [14–17].

Although glycoproteins in Table 1 possibly have the sequence to which polylactosamine-type glycans are attached, our method can not conclude this point. Therefore, glycoproteins that were assumed to be associated with the expression of polylactosamine-type glycans were identified by Western blot analysis (Fig. 5).

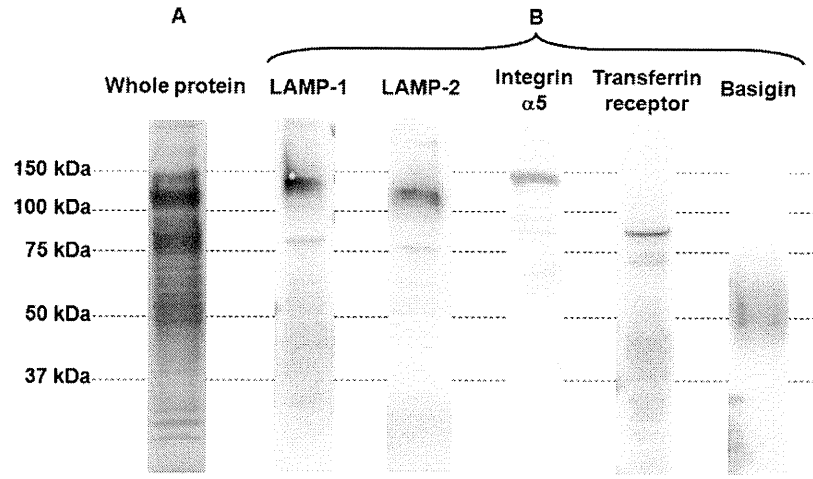

Fig. 5. Western blot and DSA lectin blot analysis of glycoproteins confirmed by shotgun analysis. (A) DSA lectin blot. (B) Western blot analysis of glycoproteins. Analytical conditions: separation gel, 10% T/2.6% C; blotting buffer: 48 mM Tris–39 mM glycine–20% methanol; blocking buffer for lectin blot, 0.05% Tween 20 in PBS; blocking buffer for Western blot, 5% skim milk–0.05% Tween 20 in PBS. Detection: HRP-DAB.

Whole protein fractions show the presence of a number of bands by DSA-lectin blot analysis (Fig. 5, lane A). The proteins identified by MASCOT analysis were confirmed by Western blot analysis (Fig. 5B). LAMP-1, LAMP-2 and integrin α5 could be clearly detected at around 100–150 kDa. Transferrin receptor protein-1 and basigin were also observed at ca. 80 kDa and 50–70 kDa, respectively. However, CD98, of which presence had been reported, was not detected (data not shown)[18]. These data are well consistent with those reported previously [13,19,20]. To verify the presence of polylactosamine-type N-glycans in these glycoproteins, we analyzed the glycans of the bands stained by Western blot analysis.

3.2. N-Glycan analysis of LAMP-1 and LAMP-2 obtained from U-937 cells by immunoprecipitation method

LAMP-1 and LAMP-2 purified by immunoprecipitation method were further separated by SDS-PAGE. And the bands at 100–150 kDa (see Fig. 5) were cut, and in-gel digested with N-glycoamidase F followed by labeling with 2AA. After neuraminidase digestion, N-glycans from LAMP-1 and LAMP-2 were analyzed by HPLC and MALDI-TOF MS. The results are shown in Fig. 6 and Table 2.

LAMP-1 and LAMP-2 contained high-mannose and complex type N-glycans abundantly. In addition, characteristic ladder peaks due to polylactosamine-type N-glycans were observed (Fig. 6). These peaks were confirmed by MALDI-TOF MS after collection of the peaks (Table 2). Fukuda's group reported the following results: LAMP-1 and LAMP-2 in colon carcinoma and human promyelocytic leukemia cells expressed tri- and tetra-antennary glycans as well as high-mannose type glycans. In addition, tetraantennary glycans having five or six lactosamine units were present abundantly in LAMP-1 and LAMP-2 molecules [8,21]. Our data clearly showed that LAMP-1 and LAMP-2 from U937 cells contained tetra-antennary glycans having elongated lactosamines (4 or 5 lactosamine units). It should be noticed that LAMP-1 contains larger polylactosamine-type N-glycans. Conventionally, the spots having polylactosamine glycans on 2D-gel were confirmed by lectin-blotting method. And the identified spots were analyzed by MS technique. Unfortunately, these techniques could not afford detailed information on glycan profiles. The proposed method in the present study focuses on specific glycopeptides having specific glycans, and will afford precise information on the changes of glycan profiles on specific glycoproteins with onset of diseases.

3.3. Comparative studies on the polylactosamine-carrying proteins present on some cancer cell lines

We compared proteins expressing polylactosamine-type glycans among various cancer cells using the methods employed for the analysis of U937 cells. Fig. 7 shows the results on the analyses of N-glycans of DSA-bound glycopeptides in A549 (human lung cancer cells), ACHN (human kidney glandular cancer cells), Jurkat (acute T cell leukemia) and MKN45 (human gastric adenocarcinoma) cells.

Characteristic ladder peaks indicate that these cell lines commonly express polylactosamine-type N-glycans. The ladder peaks observed in MKN45 cells are somewhat collapsed. This is because polylactosamine-type glycans are further modified with multiple fucose residues [3].

Based on these results, DSA-bound glycopeptides obtained from each cell line were digested with N-glycoamidase F, and the peptides having Asn-X-Ser/Thr sequences were analyzed by MS/MS analysis (Table 3). From five cancer cell lines, 25 glycoproteins in total were identified. Of the determined glycoproteins, 13 glycoproteins are CD antigens which express their own functions on the cell surface. CD98, LAMP-1 and basigin were commonly observed in all cell lines.

The sequence of SLVTQYL***NAT***GNR in CD98 was confirmed in all the examined cancer cell lines. In addition, the sequence, ***NMT***FDLPSDATVVL***NR*** (SGPK***NMT***FDLPSDATVVL***NR***) in LAMP1, was observed in four of five cancer cell lines, but the sequence was not detected in ACHN cells. The sequence, ILLTCSL***NDS***ATEVTGHR in basigin, was identified as the attaching site of polylactosamine-type glycans. These data indicate that polylactosamine-type N-glycans were abundantly observed in specific sequences. CD98, LAMP-1 and basigin were reported to be present in many cancer cells [22–24]. Especially, polylactosamine-type glycans of LAMP-1 and basigin play important roles in invasion/metastasis of cancer cells [12,21]. In addition, sialyl LewisX epitope (NeuAcα2–3Galβ1–4(Fucα1–3)GlcNACβ1–3Gal) expresses on polylactosamine-type glycans of LAMP-1 [25]. Basigin plays significant roles in tumors as well as other diseases by inducing production of matrix metalloproteinases by forming polymeric structures [13]. CD98 is observed abundantly in human tumor tissues such as melanoma, laryngeal carcinoma, lung adenocarcinoma, breast cancer, and renal cell cancers [26–29]. Functions on CD98 in relation to transport of amino acids, cell adhesion and malignant of cancer have been reported [17,29], but expression of polylactosamine-type N-glycans on CD98 is not known. The present

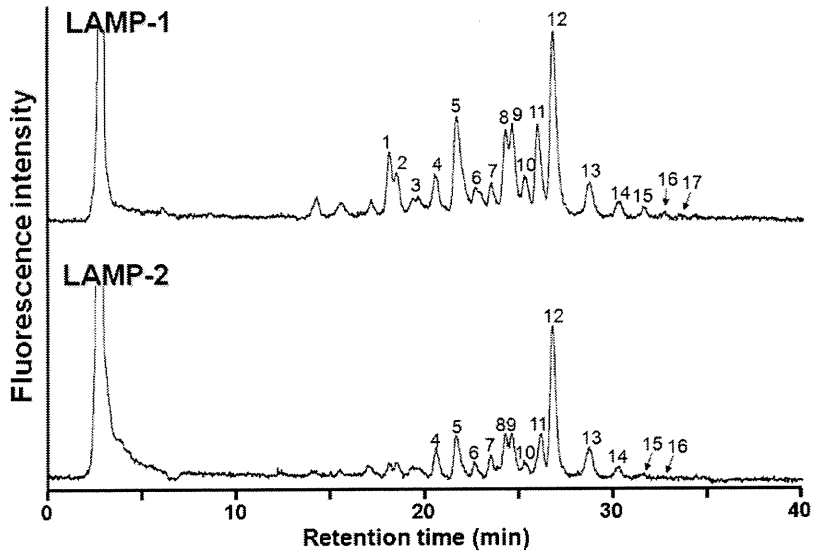

Fig. 6. HPLC analysis of N-glycans of immunoprecipitates of LAMP-1 and LAMP-2. Analytical conditions are also the same as those described in Fig. 1.

Table 2
List of oligosaccharides observed in LAMP-1 and LAMP-2.

Peak no.	Observed molecular mass		Calculated molecular mass	Monosaccharide composition
	LAMP-1	LAMP-2		
1	1356.7	1355.5		$Man_5GlcNAc_2$-2AA
2	1541.7	1542.6		$Man_3GalFucGlcNAc_3$-2AA
3	1746.9	1745.7		$Man_3GalFucGlcNAc_4$-2AA
4	1760.8	1761.0	1761.7	$Man_3Gal_2GlcNAc_4$-2AA
5	1906.9	1908.1	1907.7	$Man_3Gal_2FucGlcNAc_4$-2AA
6	1678.6	1678.9	1679.6	$Man_7GlcNAc_2$-2AA
	2110.8	2110.1	2110.8	$Man_3Gal_2FucGlcNAc_5$-2AA
7	2128.1	2126.1	2126.8	$Man_3Gal_3GlcNAc_5$-2AA
8	2271.7	2272.2	2272.8	$Man_3Gal_3FucGlcNAc_5$-2AA
9	1843.0	1840.9	1841.7	$Man_8GlcNAc_2$-2AA
	2271.7	2272.9	2272.8	$Man_3Gal_3FucGlcNAc_5$-2AA
10	2476.2	2476.0	2475.9	$Man_3Gal_3FucGlcNAc_6$-2AA
11	2002.5	2003.0	2003.7	$Man_9GlcNAc_2$-2AA
	2492.7	2492.0	2491.9	$Man_3Gal_4GlcNAc_6$-2AA
12	2637.6	2638.5	2638.0	$Man_3Gal_4FucGlcNAc_6$-2AA
13	3003.8	3003.6	3003.1	$Man_3Gal_5FucGlcNAc_7$-2AA
14	3367.8	3368.4	3368.2	$Man_3Gal_6FucGlcNAc_8$-2AA
15	3733.2	3733	43733.4	$Man_3Gal_7FucGlcNAc_9$-2AA
16	4098.3	4098	4098.5	$Man_3Gal_8FucGlcNAc_{10}$-2AA
17	4462.8		4463.6	$Man_3Gal_9FucGlcNAc_{11}$-2AA

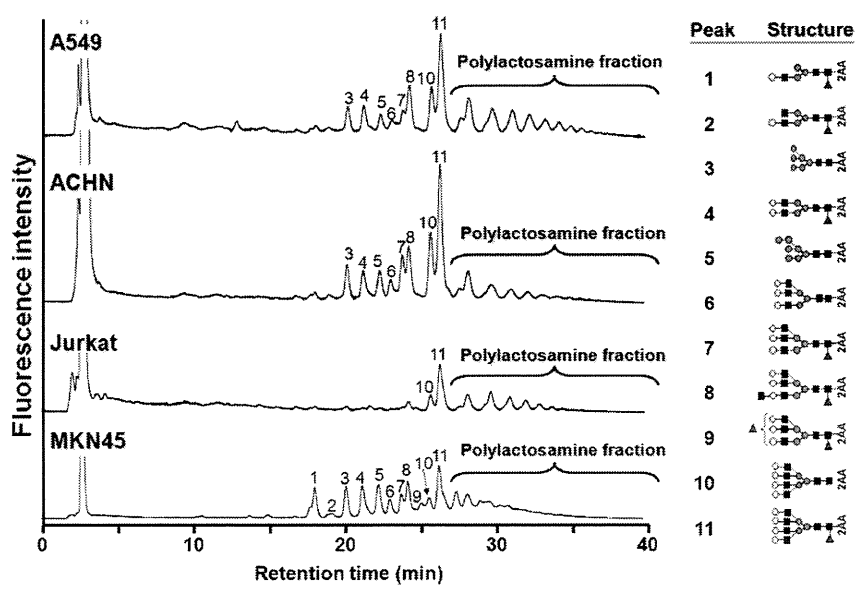

Fig. 7. HPLC analysis of N-glycans of DSA-bound glycopeptides from cancer cell.

Table 3
Comparison of possible polylactosamine-carrier proteins identified in whole protein of cancer cells.

Protein name	Jurkat	U937	MKN45	ACHN	A549
Receptor-type tyrosine-protein phosphatase C (CD45)					
YANITVDYLYNK (position: 230–241)	●				
NIETFTCDTQNITYR (position: 325–339)	●				
Integrin alpha-5 (CD49e)					
NLNNSQSDVVSFR (position: 771–783)		●			
CD59 glycoprotein					
TAVNCSSDFDACLITK (position: 40–55)	●			●	
CD63 antigen					
CCGAANYTDWEK (position: 145–156)				●	●
NRVPDSCCINVTVGCGINFNEK (position: 163–184)					●
Carcinoembryonic antigen-related cell adhesion molecule 5 (CD66e)					
EIIYPNASLLIQNIIQNDTGFYTLHVIK (position: 99–126)			●		
TLTLFNVTRNDTASYK (position: 199–214)			●		
Carcinoembryonic antigen-related cell adhesion molecule 6 (CD66c)					
ETIYPNASLLIQNVTQNDTGFYTLQVIK (position: 99–126)			●		
Transferrin receptor protein-1 (CD71)					
DFEDLYTPVNGSIVIVR (position: 242–258)		●			
4F2 cell-surface antigen heavy chain (CD98)					
DASSFLAEWQNITK (position: 355–368)	●			●	●
LLIAGTNSSDLQQILSLLESNK (position: 375–396)	●				
SLVTQYLNATGNR (position: 417–429)	●	●	●	●	●
Lysosome-associated membrane glycoprotein-1 (CD107a)					
SGPKNMTFDLPSDATVVLNR (position: 58–77)	●	●	●	●	
SSCGKENTSDPSLVIAFGR (position: 78–96)	●	●		●	
YSVQLMSFVYNLSDTHLFPNASSK (position: 111–134)			●		●
Lysosome-associated membrane glycoprotein-2 (CD107b)					
TVTISDHGTVTYNGSICGDDQNGPK (position: 63–87)	●				
VASVININPNTTHSTGSCR (position: 248–266)	●	●			
CD109 antigen					
TQDEILFSNSTR (position: 110–121)				●	
Basigin (CD147)					
ILLTCSLNDSATEVTGHR (position: 153–170)	●	●	●		●
Cation-dependent mannose-6-phosphate receptor					
LNETHIFNGSNWIMLIYK (position: 106–123)	●			●	●
Chondroitin sulfate proteoglycan 4					
GVNASAVVNVTVR (position: 2032–2044)					●
Fibronectin					
DQCIVDDITYNVNDTFHK (position: 516–533)				●	
Galectin-3-binding protein					
ALGFENATQALGR (position: 64–76)			●		
Neuroplastin					
ENGMPMDIVNTSGR (position: 275–288)					●
P2Y purinoceptor 12					
QAVDNLTSAPGNTSLCTRDYK (position: 2–22)				●	
Proactivator polypeptide					
TCDWLPKPNMSASCK (position: 93–107)					●
Solute carrier family 2, facilitated glucose transporter member 1					
VIEEFYNQTWVHR (position: 39–51)				●	
Solute carrier family 43 member 3					
DLCGPDAGPIGNATGQADCK (position: 45–64)	●				
Sortilin					
DITDLINNTFIR (position: 156–167)		●			
Synaptophysin-like protein 1					
GQTEIQVNCPPAVTENK (position: 56–72)	●				
Tetraspanin-13					
SVNPNDTCLASCVK (position: 133–146)	●				

data indicate that the common glycoproteins observed in cancer cell lines will be important markers, if N-glycans are also analyzed simultaneously.

Receptor-type tyrosine-protein phosphatase C (CD45) identified in Jurkat cells, carcinoembryonic antigen-related cell adhesion molecule 5 (CEA) in MKN45 cells, and CD63 antigens in ACHN and A549 cells are cell specific glycoproteins expressing polylactosamine-type glycans (Table 3). CD45 expresses commonly on T cells, and the attached polylactosamine-type glycans are ligands for galectin-1 [30]. CEA is observed abundantly in MKN45 cells, and closely related with cell–cell interactions through galectin-1 [31]. CEA also contains sialyl LewisX antigen [32]. Therefore, CEA molecules observed in MKN45 cells may contain Lewis antigens on their polylactosamine glycans. CD63 is observed abundantly as a specific antigen for melanoma, and contains large amount of polylactosamine-type glycans [33]. In addition, close relationship between CD63 and metastasis in lung and renal tumors has been reported [34].

The hitherto reported results described above indicate that polylactosamine-type glycans are observed in two types of glycoproteins: common glycoproteins on cancer cells and specific glycoproteins on a specific cancer cell line. Although we do not have the data on N-glycans on normal cells, the data obtained in the present study show significance of comparative studies on N-glycans among various cancer cells.

A number of proteins carrying polylactosamine-type glycans with relation to their biological functions on cancer cells have been reported. However, the studies were performed independently for each cell line, and there has been a big barrier to understand the roles of such glycan-carrying proteins as markers. As indicated in

this report, comprehensive studies using many cells at the same time will easily and clearly reveal the importance of these proteins.

4. Conclusion

In the series of studies on comprehensive analysis of glycans in cancer cells, we found that some specific glycans such as polylactosamine-type glycans are specifically and abundantly present in some cancer cells. In the present study, we proposed methods to determine specific proteins which carry specific glycans. The method is based on the following concepts: (1) finding of specific glycans expressing on specific tumors, (2) finding of specific proteins carrying these specific glycans, and (3) determination of the sequence to which specific glycans are attached.

The proposed method is well suited for the studies on these objectives, and will be a useful tool for finding glycan-based disease markers. Another project on O-glycan analysis affords complementary information on polylactosamine-type glycans in various cancer cells. Further studies on the relationship between proteins carrying polylactosamine-type N-glycans and O-glycans will lead to comprehensive and precise understanding of tumors.

References

[1] P.M. Drake, W. Cho, B. Li, A. Prakobphol, E. Johansen, N.L. Anderson, F.E. Regnier, B.W. Gibson, S.J. Fisher, Sweetening the pot: adding glycosylation to the biomarker discovery equation, Clin. Chem. 56 (2010) 223–236.
[2] M.M. Fuster, J.D. Esko, The sweet and sour of cancer: glycans as novel therapeutic targets, Nat. Rev. Cancer 5 (2005) 526–542.
[3] R. Naka, S. Kamoda, A. Ishizuka, M. Kinoshita, K. Kakehi, Analysis of total N-glycans in cell membrane fractions of cancer cells using a combination of serotonin affinity chromatography and normal phase chromatography, J. Proteome Res. 5 (2006) 88–97.
[4] K. Yamada, M. Kinoshita, T. Hayakawa, S. Nakaya, K. Kakehi, Comparative studies on the structural features of O-glycans between leukemia and epithelial cell lines, J. Proteome Res. 8 (2009) 521–537.
[5] K. Nakajima, Y. Oda, M. Kinoshita, K. Kakehi, Capillary affinity electrophoresis for the screening of post-translational modification of proteins with carbohydrates, J. Proteome Res. 2 (2003) 81–88.
[6] M. Fukuda, Cell surface glycoconjugates as onco-differentiation markers in hematopoietic cells, Biochim. Biophys. Acta 780 (1985) 119–150.
[7] S.R. Carlsson, M. Fukuda, The polylactosaminoglycans of human lysosomal membrane glycoproteins lamp-1 and lamp-2. Localization on the peptide backbones, J. Biol. Chem. 265 (1990) 20488–20495.
[8] N. Lee, W.C. Wang, M. Fukuda, Granulocytic differentiation of HL-60 cells is associated with increase of poly-N-acetyllactosamine in Asn-linked oligosaccharides attached to human lysosomal membrane glycoproteins, J. Biol. Chem. 265 (1990) 20476–20487.
[9] A. Togayachi, Y. Kozono, H. Ishida, S. Abe, N. Suzuki, Y. Tsunoda, K. Hagiwara, A. Kuno, T. Ohkura, N. Sato, T. Sato, J. Hirabayashi, Y. Ikehara, K. Tachibana, H. Narimatsu, Polylactosamine on glycoproteins influences basal levels of lymphocyte and macrophage activation, Proc. Natl. Acad. Sci. U.S.A. 104 (2007) 15829–15834.
[10] Q. Sun, X. Kang, Y. Zhang, H. Zhou, Z. Dai, W. Lu, X. Zhou, X. Liu, P. Yang, Y. Liu, DSA affinity glycoproteome of human liver tissue, Arch. Biochem. Biophys. 484 (2009) 24–29.
[11] J. Gu, T. Isaji, Y. Sato, Y. Kariya, T. Fukuda, Importance of N-glycosylation on alpha5beta1 integrin for its biological functions, Biol. Pharm. Bull. 32 (2009) 780–785.
[12] S. Laferte, J.W. Dennis, Purification of two glycoproteins expressing beta 1–6 branched Asn-linked oligosaccharides from metastatic tumour cells, Biochem. J. 259 (1989) 569–576.
[13] W. Tang, S.B. Chang, M.E. Hemler, Links between CD147 function, glycosylation, and caveolin-1, Mol. Biol. Cell 15 (2004) 4043–4050.
[14] R. Chen, X. Jiang, D. Sun, G. Han, F. Wang, M. Ye, L. Wang, H. Zou, Glycoproteomics analysis of human liver tissue by combination of multiple enzyme digestion and hydrazide chemistry, J. Proteome Res. 8 (2009) 651–661.
[15] T. Liu, W.J. Qian, M.A. Gritsenko, D.G. Camp 2nd, M.E. Monroe, R.J. Moore, R.D. Smith, Human plasma N-glycoproteome analysis by immunoaffinity subtraction, hydrazide chemistry, and mass spectrometry, J. Proteome Res. 4 (2005) 2070–2080.
[16] B. Wollscheid, D. Bausch-Fluck, C. Henderson, R. O'Brien, M. Bibel, R. Schiess, R. Aebersold, J.D. Watts, Mass-spectrometric identification and relative quantification of N-linked cell surface glycoproteins, Nat. Biotechnol. 27 (2009) 378–386.
[17] Y. Yan, S. Vasudevan, H.T. Nguyen, D. Merlin, Intestinal epithelial CD98: an oligomeric and multifunctional protein, Biochim. Biophys. Acta 1780 (2008) 1087–1092.
[18] J.Y. Cho, D.A. Fox, V. Horejsi, K. Sagawa, K.M. Skubitz, D.R. Katz, B. Chain, The functional interactions between CD98, beta1-integrins, and CD147 in the induction of U937 homotypic aggregation, Blood 98 (2001) 374–382.
[19] H.B. Guo, I. Lee, M. Kamar, S.K. Akiyama, M. Pierce, Aberrant N-glycosylation of beta1 integrin causes reduced alpha5beta1 integrin clustering and stimulates cell migration, Cancer Res. 62 (2002) 6837–6845.
[20] L. Li, C.J. Fang, J.C. Ryan, E.C. Niemi, J.A. Lebron, P.J. Bjorkman, H. Arase, F.M. Torti, S.V. Torti, M.C. Nakamura, W.E. Seaman, Binding and uptake of H-ferritin are mediated by human transferrin receptor-1, Proc. Natl. Acad. Sci. U.S.A. 107 (2010) 3505–3510.
[21] O. Saitoh, W.C. Wang, R. Lotan, M. Fukuda, Differential glycosylation and cell surface expression of lysosomal membrane glycoproteins in sublines of a human colon cancer exhibiting distinct metastatic potentials, J. Biol. Chem. 267 (1992) 5700–5711.
[22] S.R. Carlsson, J. Roth, F. Piller, M. Fukuda, Isolation and characterization of human lysosomal membrane glycoproteins, h-lamp-1 and h-lamp-2. Major sialoglycoproteins carrying polylactosaminoglycan, J. Biol. Chem. 263 (1988) 18911–18919.
[23] L.C. Bordador, X. Li, B. Toole, B. Chen, J. Regezi, L. Zardi, Y. Hu, D.M. Ramos, Expression of emmprin by oral squamous cell carcinoma, Int. J. Cancer 85 (2000) 347–352.
[24] K. Nabeshima, J. Suzumiya, M. Nagano, K. Ohshima, B.P. Toole, K. Tamura, H. Iwasaki, M. Kikuchi, Emmprin, a cell surface inducer of matrix metalloproteinases (MMPs), is expressed in T-cell lymphomas, J. Pathol. 202 (2004) 341–351.
[25] R. Sawada, J.B. Lowe, M. Fukuda, E-selectin-dependent adhesion efficiency of colonic carcinoma cells is increased by genetic manipulation of their cell surface lysosomal membrane glycoprotein-1 expression levels, J. Biol. Chem. 268 (1993) 12675–12681.
[26] F. Esteban, F. Ruiz-Cabello, A. Concha, M. Perez Ayala, M. Delgado, F. Garrido, Relationship of 4F2 antigen with local growth and metastatic potential of squamous cell carcinoma of the larynx, Cancer 66 (1990) 1493–1498.
[27] S. Esseghir, J.S. Reis-Filho, A. Kennedy, M. James, M.J. O'Hare, R. Jeffery, R. Poulsom, C.M. Isacke, Identification of transmembrane proteins as potential prognostic markers and therapeutic targets in breast cancer by a screen for signal sequence encoding transcripts, J. Pathol. 210 (2006) 420–430.
[28] K. Kaira, N. Oriuchi, H. Imai, K. Shimizu, N. Yanagitani, N. Sunaga, T. Hisada, S. Tanaka, T. Ishizuka, Y. Kanai, H. Endou, T. Nakajima, M. Mori, l-type amino acid transporter 1 and CD98 expression in primary and metastatic sites of human neoplasms, Cancer Sci. 99 (2008) 2380–2386.
[29] G.W. Prager, M. Poettler, M. Schmidinger, P.R. Mazal, M. Susani, C.C. Zielinski, A. Haitel, CD98hc (SLC3A2), a novel marker in renal cell cancer, Eur. J. Clin. Invest. 39 (2009) 304–310.
[30] M. Amano, M. Galvan, J. He, L.G. Baum, The ST6Gal I sialyltransferase selectively modifies N-glycans on CD45 to negatively regulate galectin-1-induced CD45 clustering, phosphatase modulation, and T cell death, J. Biol. Chem. 278 (2003) 7469–7475.
[31] D.W. Ohannesian, D. Lotan, R. Lotan, Concomitant increases in galectin-1 and its glycoconjugate ligands (carcinoembryonic antigen, lamp-1, and lamp-2) in cultured human colon carcinoma cells by sodium butyrate, Cancer Res. 54 (1994) 5992–6000.
[32] K. Yamashita, K. Totani, M. Kuroki, Y. Matsuoka, I. Ueda, A. Kobata, Structural studies of the carbohydrate moieties of carcinoembryonic antigens, Cancer Res. 47 (1987) 3451–3459.
[33] A. Engering, L. Kuhn, D. Fluitsma, E. Hoefsmit, J. Pieters, Differential post-translational modification of CD63 molecules during maturation of human dendritic cells, Eur. J. Biochem. 270 (2003) 2412–2420.
[34] M.S. Kwon, S.H. Shin, S.H. Yim, K.Y. Lee, H.M. Kang, T.M. Kim, Y.J. Chung, CD63 as a biomarker for predicting the clinical outcomes in adenocarcinoma of lung, Lung Cancer 57 (2007) 46–53.

Research Article

EASL EUROPEAN ASSOCIATION FOR THE STUDY OF THE LIVER | JOURNAL OF HEPATOLOGY

Generation of metabolically functioning hepatocytes from human pluripotent stem cells by FOXA2 and HNF1α transduction

Kazuo Takayama[1,2], Mitsuru Inamura[1,2], Kenji Kawabata[2,3], Michiko Sugawara[4], Kiyomi Kikuchi[4], Maiko Higuchi[2], Yasuhito Nagamoto[1,2], Hitoshi Watanabe[1,2], Katsuhisa Tashiro[2], Fuminori Sakurai[1], Takao Hayakawa[5,6], Miho Kusuda Furue[7,8], Hiroyuki Mizuguchi[1,2,9,*]

[1]*Laboratory of Biochemistry and Molecular Biology, Graduate School of Pharmaceutical Sciences, Osaka University, Osaka 565-0871, Japan;* [2]*Laboratory of Stem Cell Regulation, National Institute of Biomedical Innovation, Osaka 567-0085, Japan;* [3]*Laboratory of Biomedical Innovation, Graduate School of Pharmaceutical Sciences, Osaka University, Osaka 565-0871, Japan;* [4]*Tsukuba Laboratories, Eisai Co., Ltd., Ibaraki 300-2635, Japan;* [5]*Pharmaceutics and Medical Devices Agency, Tokyo 100-0013, Japan;* [6]*Pharmaceutical Research and Technology Institute, Kinki University, Osaka 577-8502, Japan;* [7]*Laboratory of Cell Cultures, Department of Disease Bioresources Research, National Institute of Biomedical Innovation, Osaka 567-0085, Japan;* [8]*Laboratory of Cell Processing, Institute for Frontier Medical Sciences, Kyoto University, Kyoto 606-8507, Japan;* [9]*The Center for Advanced Medical Engineering and Informatics, Osaka University, Osaka 565-0871, Japan*

Background & Aims: Hepatocyte-like cells differentiated from human embryonic stem cells (hESCs) and induced pluripotent stem cells (hiPSCs) can be utilized as a tool for screening for hepatotoxicity in the early phase of pharmaceutical development. We have recently reported that hepatic differentiation is promoted by sequential transduction of SOX17, HEX, and HNF4α into hESC- or hiPSC-derived cells, but further maturation of hepatocyte-like cells is required for widespread use of drug screening.
Methods: To screen for hepatic differentiation-promoting factors, we tested the seven candidate genes related to liver development.
Results: The combination of two transcription factors, FOXA2 and HNF1α, promoted efficient hepatic differentiation from hESCs and hiPSCs. The expression profile of hepatocyte-related genes (such as genes encoding cytochrome P450 enzymes, conjugating enzymes, hepatic transporters, and hepatic nuclear receptors) achieved with FOXA2 and HNF1α transduction was comparable to that obtained in primary human hepatocytes. The hepatocyte-like cells generated by FOXA2 and HNF1α transduction exerted various hepatocyte functions including albumin and urea secretion, and the uptake of indocyanine green and low density lipoprotein. Moreover, these cells had the capacity to metabolize all nine tested drugs and were successfully employed to evaluate drug-induced cytotoxicity.
Conclusions: Our method employing the transduction of FOXA2 and HNF1α represents a useful tool for the efficient generation of metabolically functional hepatocytes from hESCs and hiPSCs, and the screening of drug-induced cytotoxicity.

Keywords: FOXA2; HNF1α; Hepatocytes; Adenovirus; Drug screening; Drug metabolism; hESCs; hiPSCs.
Received 14 November 2011; received in revised form 31 March 2012; accepted 4 April 2012; available online 29 May 2012
* Corresponding author. Address: Laboratory of Biochemistry and Molecular Biology, Graduate School of Pharmaceutical Sciences, Osaka University, 1-6 Yamadaoka, Suita, Osaka 565-0871, Japan. Tel.: +81 6 6879 8185; fax: +81 6 6879 8186.
E-mail address: mizuguch@phs.osaka-u.ac.jp (H. Mizuguchi).

Introduction

Hepatocyte-like cells differentiated from human embryonic stem cells (hESCs) [1] or human induced pluripotent stem cells (hiPSCs) [2] have more advantages than primary human hepatocytes (PHs) for drug screening. While application of PHs in drug screening has been hindered by lack of cellular growth, loss of function, and de-differentiation *in vitro* [3], hESC- or hiPSC-derived hepatocyte-like cells (hESC-hepa or hiPSC-hepa, respectively) have potential to solve these problems.

Hepatic differentiation from hESCs and hiPSCs can be divided into four stages: definitive endoderm (DE) differentiation, hepatic commitment, hepatic expansion, and hepatic maturation. Various growth factors are required to mimic liver development [4] and to promote hepatic differentiation. Previously, we showed that transduction of transcription factors in addition to treatment with optimal growth factors was effective to enhance hepatic differentiation [5–7]. An almost homogeneous hepatocyte population was obtained by sequential transduction of SOX17, HEX, and HNF4α into hESC- or hiPSCs-derived cells [7]. However, further maturation of the hESC-hepa and hiPSC-hepa is required for widespread use of drug screening because the drug metabolism capacity of these cells was not sufficient.

In some previous reports, hESC-hepa and hiPSC-hepa have been characterized for their hepatocyte functions in numerous ways, including functional assessment such as glycogen storage and low density lipoprotein (LDL) uptake [7]. To make a more precise judgment as to whether hESC-hepa and hiPSC-hepa can be applied to drug screening, it is more important to assess cytochrome P450 (CYP) induction potency and drug metabolism capacity rather than general hepatocyte function. Although Duan *et al.* have examined the drug metabolism capacity of hESC-hepa, drug metabolites were measured at 24 or 48 h [8]. To precisely

estimate the drug metabolism capacity, the amount of metabolites must be measured during the time when production of metabolites is linearly detected (generally before 24 h). To the best of our knowledge, there have been few reports that have examined various drugs metabolism capacity of hESC-hepa and hiPSC-hepa in detail.

In the present study, seven candidate genes (*FOXA2*, *HEX*, *HNF1α*, *HNF1β*, *HNF4α*, *HNF6*, and *SOX17*) were transduced into each stage of hepatic differentiation from hESCs by using an adenovirus (Ad) vector to screen for hepatic differentiation-promoting factors. Then, hepatocyte-related gene expression profiles and hepatocyte functions in hESC-hepa and hiPSC-hepa generated by the optimized protocol, were examined to investigate whether these cells have PHs characteristics. We used nine drugs, which are metabolized by various CYP enzymes and UDP-glucuronosyltransferases (UGTs), to determine whether the hESC-hepa and hiPSC-hepa have drug metabolism capacity. Furthermore, hESC-hepa and hiPSC-hepa were examined to determine whether these cells may be applied to evaluate drug-induced cytotoxicity.

Materials and methods

In vitro differentiation

Before the initiation of cellular differentiation, the medium of hESCs and hiPSCs was exchanged for a defined serum-free medium, hESF9, and cultured as previously reported [9]. The differentiation protocol for the induction of DE cells, hepatoblasts, and hepatocytes was based on our previous report with some modifications [5,6]. Briefly, in mesendoderm differentiation, hESCs and hiPSCs were dissociated into single cells by using Accutase (Millipore) and cultured for 2 days on Matrigel (BD biosciences) in differentiation hESF-DIF medium which contains 100 ng/ml Activin A (R&D Systems) and 10 ng/ml bFGF (hESF-DIF medium, Cell Science & Technology Institute; differentiation hESF-DIF medium was supplemented with 10 μg/ml human recombinant insulin, 5 μg/ml human apotransferrin, 10 μM 2-mercaptoethanol, 10 μM ethanolamine, 10 μM sodium selenite, and 0.5 mg/ml bovine serum albumin, all from Sigma). To generate DE cells, mesendoderm cells were transduced with 3000 VP/cell of Ad-FOXA2 for 1.5 h on day 2 and cultured until day 6 on Matrigel in differentiation hESF-DIF medium supplemented with 100 ng/ml Activin A and 10 ng/ml bFGF. For induction of hepatoblasts, the DE cells were transduced with each 1500 VP/cell of Ad-FOXA2 and Ad-HNF1α for 1.5 h on day 6 and cultured for 3 days on Matrigel in hepatocyte culture medium (HCM, Lonza) supplemented with 30 ng/ml bone morphogenetic protein 4 (BMP4, R&D Systems) and 20 ng/ml FGF4 (R&D Systems). In hepatic expansion, the hepatoblasts were transduced with each 1500 VP/cell of Ad-FOXA2 and Ad-HNF1α for 1.5 h on day 9 and cultured for 3 days on Matrigel in HCM supplemented with 10 ng/ml hepatocyte growth factor (HGF), 10 ng/ml FGF1, 10 ng/ml FGF4, and 10 ng/ml FGF10 (all from R&D Systems). In hepatic maturation, cells were cultured for 8 days on Matrigel in L15 medium (Invitrogen) supplemented with 8.3% tryptose phosphate broth (BD biosciences), 10% FBS (Vita), 10 μM hydrocortisone 21-hemisuccinate (Sigma), 1 μM insulin, 25 mM $NaHCO_3$ (Wako), 20 ng/ml HGF, 20 ng/ml Oncostatin M (OsM, R&D systems), and 10^{-6} M Dexamethasone (DEX, Sigma).

Results

Recently, we showed that the sequential transduction of SOX17, HEX, and HNF4α into hESC-derived mesendoderm, DE, and hepatoblasts, respectively, leads to efficient generation of the hESC-hepa [5–7]. In the present study, to further improve the differentiation efficiency towards hepatocytes, we screened for hepatic differentiation-promoting transcription factors. Seven candidate genes involved in liver development were selected. We then examined the function of the hESC-hepa and hiPSC-hepa generated by the optimized protocol for pharmaceutical use in detail.

Efficient hepatic differentiation by Ad-FOXA2 and Ad-HNF1α transduction

To perform efficient DE differentiation, T-positive hESC-derived mesendoderm cells (day 2) (Supplementary Fig. 1) were transduced with Ad vector expressing various transcription factors (Ad-FOXA2, Ad-HEX, Ad-HNF1α, Ad-HNF1β, Ad-HNF4α, Ad-HNF6, and Ad-SOX17 were used in this study). We ascertained the expression of *FOXA2*, *HEX*, *HNF1α*, *HNF1β*, *HNF4α*, *HNF6*, or *SOX17* in Ad-FOXA2-, Ad-HEX-, Ad-HNF1α-, Ad-HNF1β-, Ad-HNF4α-, Ad-HNF6-, or Ad-SOX17-transduced cells, respectively (Supplementary Fig. 2). We also verified that there was no cytotoxicity of the cells transduced with Ad vector until the total amount of Ad vector reached 12,000 VP/cell (Supplementary Fig. 3). Each transcription factor was expressed in hESC-derived mesendoderm cells on day 2 by using Ad vector, and the efficiency of DE differentiation was examined (Fig. 1A). The DE differentiation efficiency based on CXCR4-positive cells was the highest when Ad-SOX17 or Ad-FOXA2 were transduced (Fig. 1B). To investigate the difference between Ad-FOXA2-transduced cells and Ad-SOX17-transduced cells, gene expression levels of markers of undifferentiated cells, mesendoderm cells, DE cells, and extraembryonic endoderm cells were examined (Fig. 1C). The expression levels of extraembryonic endoderm markers of Ad-SOX17-transduced cells were higher than those of Ad-FOXA2-transduced cells. Therefore, we concluded that FOXA2 transduction is suitable for use in selective DE differentiation.

To promote hepatic commitment, various transcription factors were transduced into DE cells and the resulting phenotypes were examined on day 9 (Fig. 1D). Nearly 100% of the population of Ad-FOXA2-transduced cells and Ad-HNF1α-transduced cells was α-fetoprotein (AFP)-positive (Fig. 1E). We expected that hepatic commitment would be further accelerated by combining FOXA2 and HNF1α transduction. The DE cells were transduced with both Ad-FOXA2 and Ad-HNF1α, and then the gene expression levels of *CYP3A7* [10], which is a marker of fetal hepatocytes, were evaluated (Fig. 1F). When both Ad-FOXA2 and Ad-HNF1α were transduced into DE cells, the promotion of hepatic commitment was greater than in Ad-FOXA2-transduced cells or Ad-HNF1α-transduced cells.

To promote hepatic expansion and maturation, we transduced various transcription factors into hepatoblasts on day 9 and 12 and the resulting phenotypes were examined on day 20 (Fig. 1G). We ascertained that the hepatoblast population was efficiently expanded by addition of HGF, FGF1, FGF4, and FGF10 (Supplementary Fig. 4). The hepatic differentiation efficiency based on asialoglycoprotein receptor 1 (ASGR1)-positive cells was measured on day 20, demonstrating that FOXA2, HNF1α, and HNF4α transduction could promote efficient hepatic maturation (Fig. 1H). To investigate the phenotypic difference between Ad-FOXA2-, Ad-HNF1α-, and Ad-HNF4α-transduced cells, gene expression levels of early hepatic markers, mature hepatic markers, and biliary markers were examined (Fig. 1I). Gene expression levels of mature hepatic markers were up-regulated by FOXA2, HNF1α, or HNF4α transduction. FOXA2 transduction strongly upregulated gene expression levels of both early hepatic markers and mature hepatic markers, while HNF1α or HNF4α transduc-

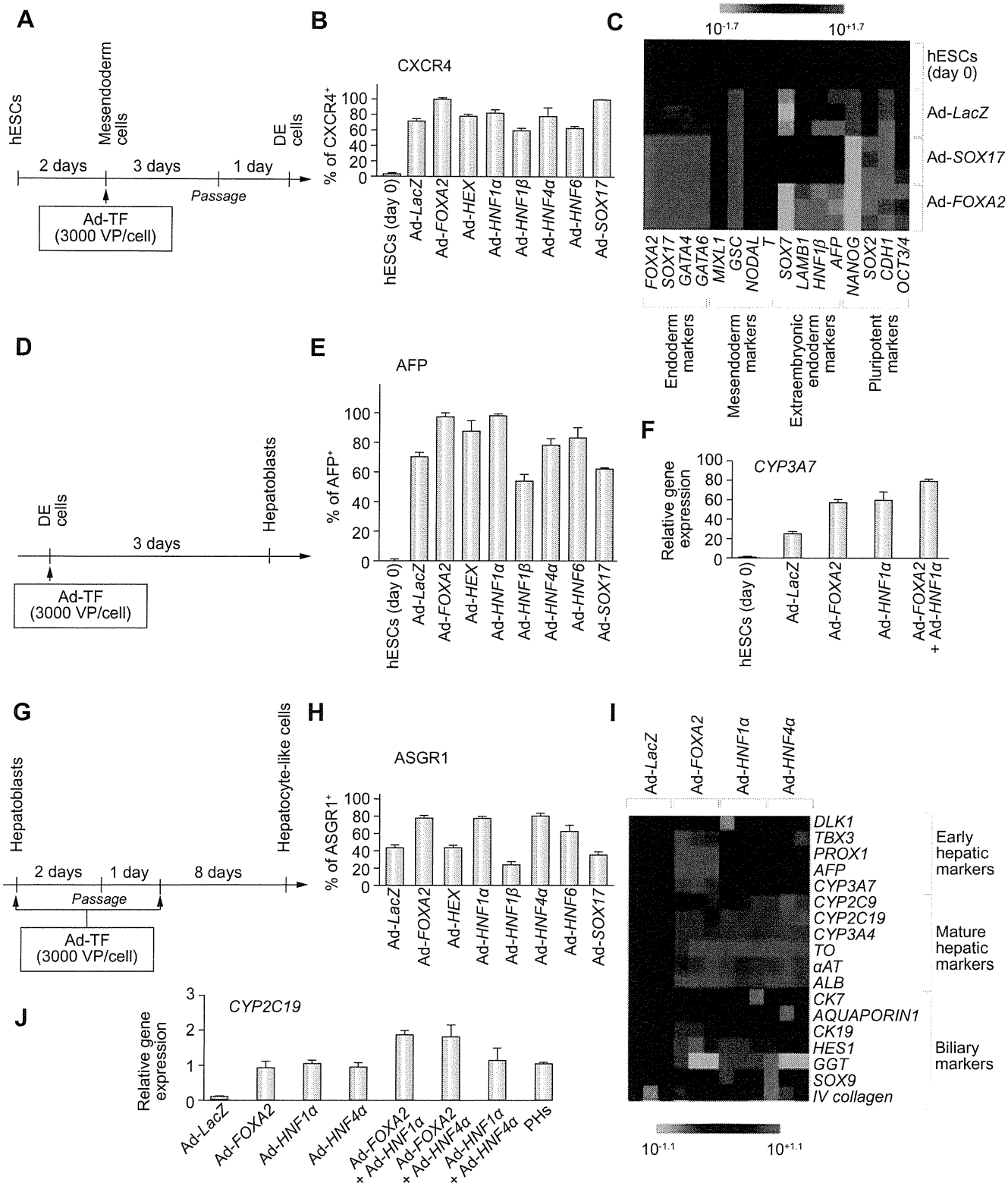

Fig. 1. Efficient hepatic differentiation from hESCs by FOXA2 and HNF1α transduction. (A) The schematic protocol describes the strategy for DE differentiation from hESCs (H9). Mesendoderm cells (day 2) were transduced with 3000 VP/cell of transcription factor (TF)-expressing Ad vector (Ad-TF) for 1.5 h and cultured as described in Fig. 2A. (B) On day 5, the efficiency of DE differentiation was measured by estimating the percentage of CXCR4-positive cells using FACS analysis. (C) The gene expression profiles were examined on day 5. (D) Schematic protocol describing the strategy for hepatoblast differentiation from DE. DE cells (day 6) were transduced with 3000 VP/cell of Ad-TF for 1.5 h and cultured as described in Fig. 2A. (E) On day 9, the efficiency of hepatoblast differentiation was measured by estimating the percentage of AFP-positive

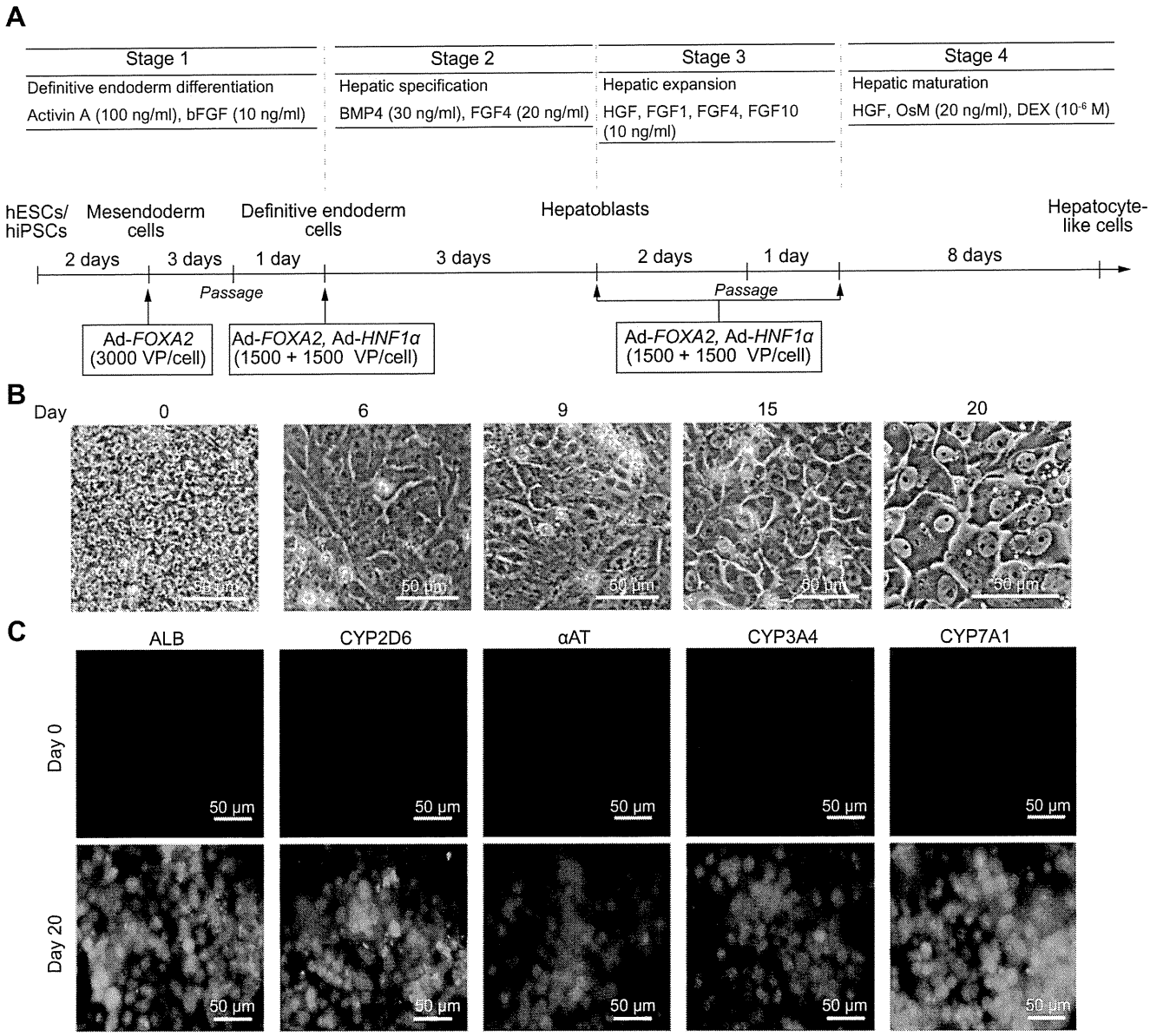

Fig. 2. Hepatic differentiation of hESCs and hiPSCs by FOXA2 and HNF1α transduction. (A) The differentiation procedure of hESCs and hiPSCs into hepatocytes via DE cells and hepatoblasts is schematically shown. Details of the hepatic differentiation procedure are described in Materials and methods. (B) Sequential morphological changes (day 0–20) of hESCs (H9) differentiated into hepatocytes are shown. (C) The expression of the hepatocyte markers (ALB, CYP2D6, αAT, CYP3A4, and CYP7A1, all green) was examined by immunohistochemistry on day 0 and 20. Nuclei were counterstained with DAPI (blue).

tion did not up-regulate the gene expression levels of early hepatic markers. Next, multiple transduction of transcription factors was performed to promote further hepatic maturation. The combination of Ad-FOXA2 and Ad-HNF1α transduction and the combination of Ad-FOXA2 and Ad-HNF4α transduction result in the most efficient hepatic maturation, judged from the gene expression levels of *CYP2C19* (Fig. 1J). This may happen because the mixture of immature hepatocytes and mature hepatocytes coor-

cells using FACS analysis. (F) The gene expression level of *CYP3A7* was measured by real-time RT-PCR on day 9. On the *y* axis, the gene expression level of *CYP3A7* in hESCs (day 0) was taken as 1.0. (G) The schematic protocol describes the strategy for hepatic differentiation from hepatoblasts. Hepatoblasts (day 9) were transduced with 3000 VP/cell of Ad-TF for 1.5 h and cultured as described in Fig. 2A. (H) On day 20, the efficiency of hepatic differentiation was measured by estimating the percentage of ASGR1-positive cells using FACS analysis. The detail results of FACS analysis are shown in Supplementary Table 1. (I) Gene expression profiles were examined on day 20. (J) Hepatoblasts (day 9) were transduced with 3000 VP/cell of Ad-TFs (in the case of combination transduction of two types of Ad vector, 1500 VP/cell of each Ad-TF was transduced) for 1.5 h and cultured. Gene expression levels of *CYP2C19* were measured by real-time RT-PCR on day 20. On the *y* axis, the gene expression level of *CYP2C19* in PHs, which were cultured for 48 h after the cells were plated, was taken as 1.0. All data are represented as mean ± SD (n = 3).

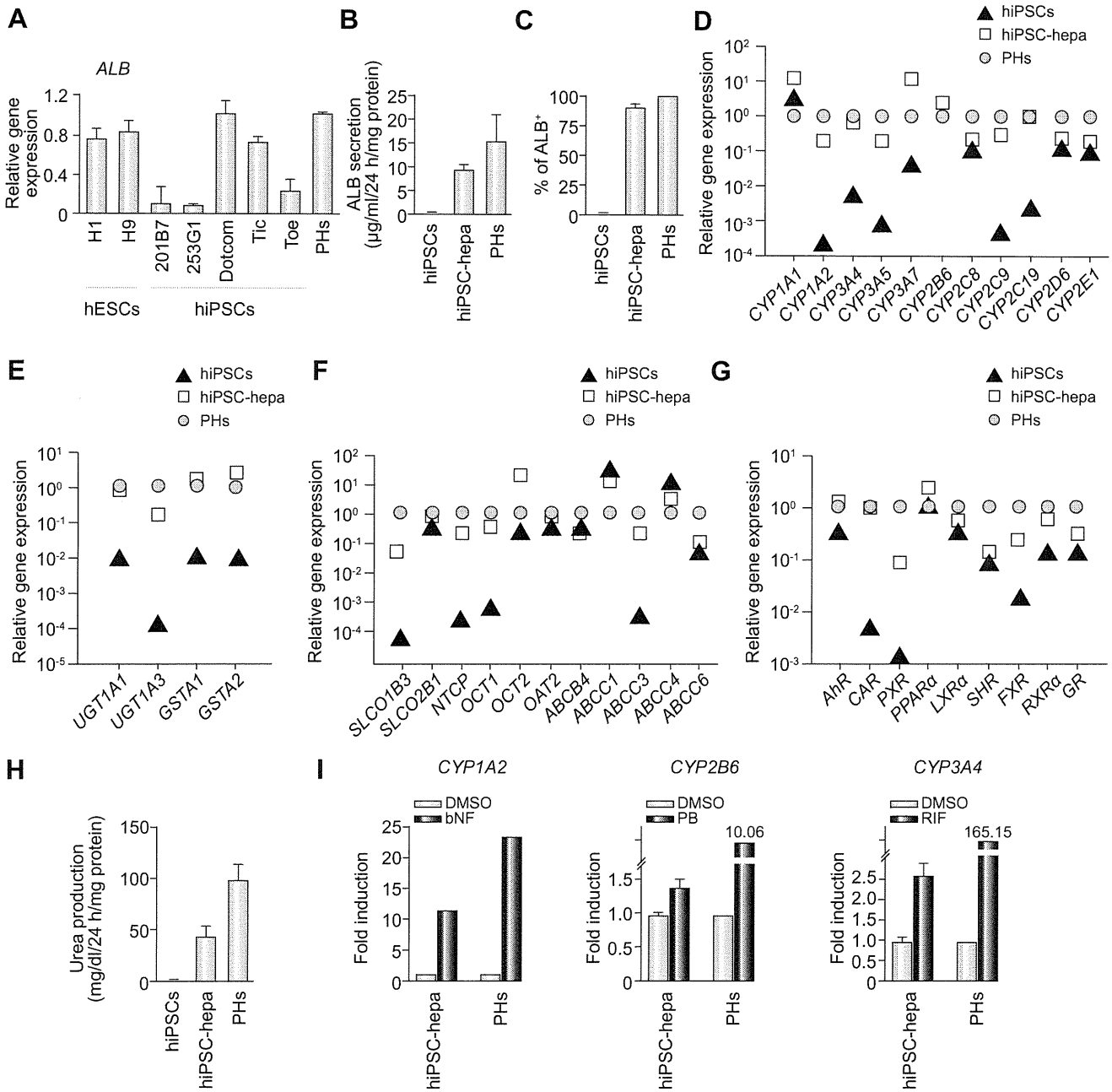

Fig. 3. The hepatic characterization of hiPSC-hepa. hESCs (H1 and H9) and hiPSCs (201B7, 253G1, Dotcom, Tic, and Toe) were differentiated into hepatocyte-like cells as described in Fig. 2A. (A) On day 20, the gene expression level of *ALB* was examined by real-time RT-PCR. On the *y* axis, the gene expression level of *ALB* in PHs, which were cultured for 48 h after cells were plated, was taken as 1.0. (B–I) hiPSCs (Dotcom) were differentiated into hepatocyte-like cells as described in Fig. 2A. (B) The amount of ALB secretion was examined by ELISA in hiPSCs, hiPSC-hepa, and PHs. (C) hiPSCs, hiPSC-hepa, and PHs were subjected to immunostaining with anti-ALB antibodies, and then the percentage of ALB-positive cells was examined by flow cytometry. (D–G) The gene expression levels of CYP enzymes (D), conjugating enzymes (E), hepatic transporters (F), and hepatic nuclear receptors (G) were examined by real-time RT-PCR in hiPSCs, hiPSC-hepa, and PHs. On the *y* axis, the expression level of PHs is indicated. (H) The amount of urea secretion was examined in hiPSCs, hiPSC-hepa, and PHs. (I) Induction of *CYP1A2*, *2B6*, or *3A4* by DMSO or inducer (bNF, PB, or RIF) of hiPSC-hepa and PHs, cultured for 48 h after the cells were plated, was examined. On the y axis, the gene expression levels of *CYP1A2*, *2B6*, or *3A4* in DMSO-treated cells, which were cultured for 48 h, were taken as 1.0. All data are represented as mean ± SD (n = 3).

dinately works to induce hepatocyte functions. Taken together, efficient hepatic differentiation could be promoted by using the combination of FOXA2 and HNF1α transduction at the optimal stage of differentiation (Fig. 2A). At the stage of hepatic expansion and maturation, Ad-HNF4α can be substituted for Ad-HNF1α (Fig. 1J). Interestingly, cell growth was delayed by FOXA2 and HNF4α transduction (Supplementary Fig. 5). This delay in cell proliferation might be due to promoted maturation by FOXA2 and HNF1α transduction. As the hepatic differentiation proceeds, the morphology of hESCs gradually changed into a typical hepatocyte morphology, with distinct round nuclei and a polygonal shape (Fig. 2B), and the expression levels of hepatic markers

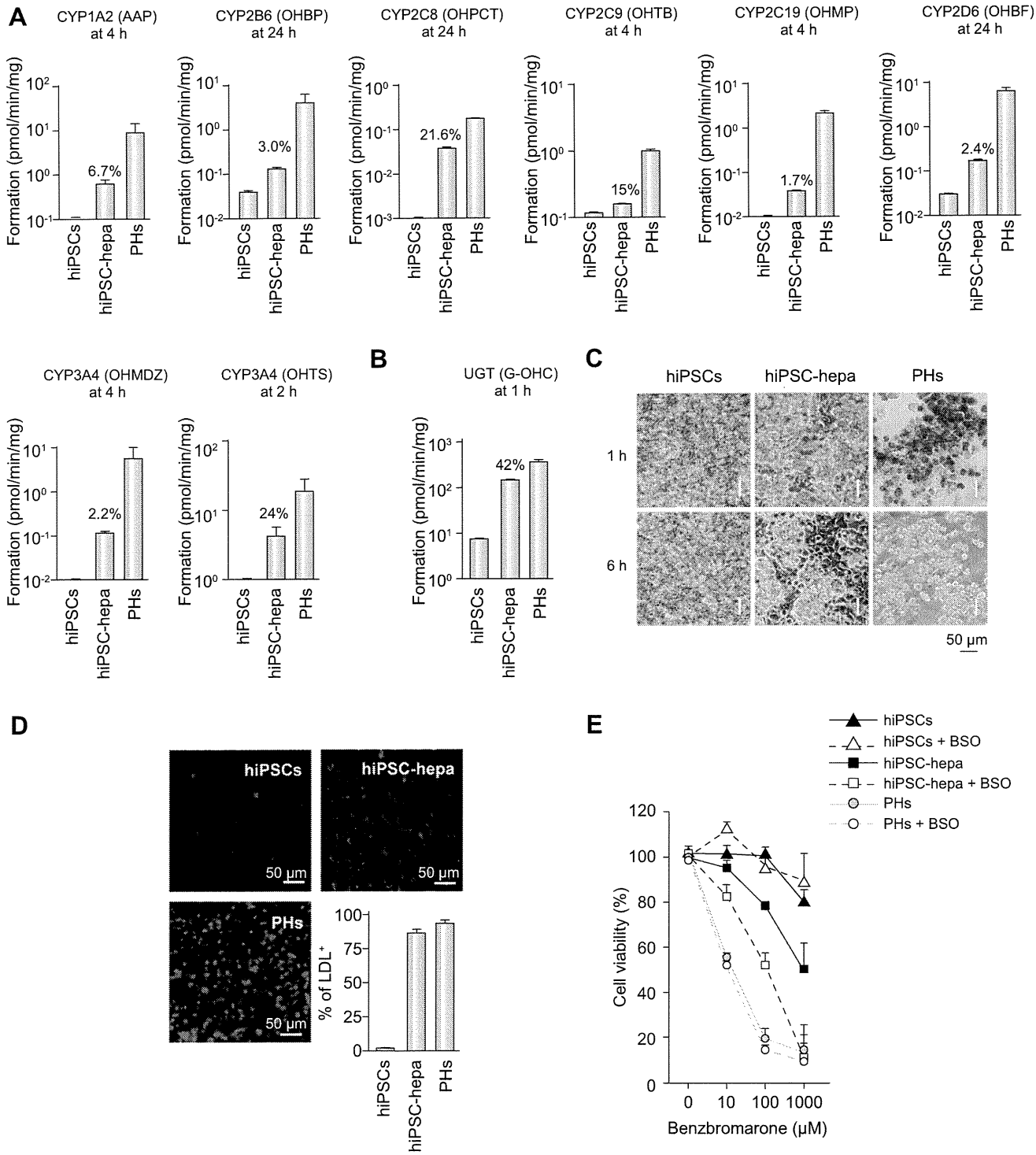

Fig. 4. Evaluation of the drug metabolism capacity and hepatic transporter activity of hiPSC-hepa. hiPSCs (Dotcom) were differentiated into hepatocytes as described in Fig. 2A. (A and B) Quantitation of metabolites in hiPSCs, hiPSC-hepa, and PHs, which were cultured for 48 h after the cells were plated, was examined by treating nine substrates (Phenacetin, Bupropion, Paclitazel, Tolbtamide, *S*-mephenytoin, Bufuralol, Midazolam, Testosterone, and Hydroxyl coumarin; these compounds are substrates for CYP1A2, 2B6, 2C8, 2C9, 2C19, 2D6, 3A4, 3A4 (A) and UGT (B), respectively), and then supernatants were collected at the indicated time. The quantity of metabolites (Acetaminophen [AAP], Hydroxybupropion [OHBP], 6α-hydroxypaclitaxel [OHPCT], Hydroxytolbutamide [OHTB], 4′-hydroxymephenytoin [OHMP], 1′-hydroxybufuralol [OHBF], 1′-hydroxymidazolam [OHMDZ], 6β-hydroxytestosterone [OHTS], 7-Hydroxycoumarin glucuronide [G-OHC], respectively) was measured by LC-MS/MS. The ratios of the activity levels in hiPSC-hepa to the activity levels in PHs rate are indicated in the graph. (C) hiPSCs, hiPSC-hepa, and PHs were examined for their ability to take up ICG (top) and release it 6 h thereafter (bottom). (D) hiPSCs, hiPSC-hepa, and PHs were cultured with medium containing Alexa-Flour 488-labeled LDL (green) for 1 h, and immunohistochemistry was performed. Nuclei were counterstained with DAPI (blue). The percentage of LDL-positive cells was also measured by FACS analysis. (E)